Alma Mater Studiorum – Università di Bologna

DOTTORATO DI RICERCA IN

CHIMICA

Ciclo XXIX

Settore Concorsuale di afferenza: 03/B1

Settore Scientifico disciplinare: CHIM/03

Synthesis and characterization of new luminescent complexes based on Copper(I) Iodide

Presentata da: **FARINELLA FRANCESCO**

Coordinatore Dottorato **Relatore**

Prof. Aldo Roda **Prof. Dario Braga**

Esame finale anno 2017

Sommario

'Some men see things as they are and say why.
I dream things that never were and say why not.'
- Robert F. Kennedy

Dott. Francesco Farinella

Supervisore: Prof. Dario Braga

Curriculum: Scienze Chimiche

Indirizzo: Chimica Inorganica

Titolo della tesi: Synthesis and characterization of new luminescent complexes based on Copper(I) iodide

Since the beginning of its Ph.D, Francesco Farinella's research efforts have been directed to the quest for high efficiency and low cost luminescent complexes by designing so as to increase the quantum yield and to find the link between the luminescent and the structural properties. The Ph.D project was mainly focused on two lines of research, including the design, synthesis and full characterization of copper iodide based luminescent complexes and the determination of the crystal structures from both powder diffraction and single crystal diffraction data. CuI derivatives have been studied since the luminescent properties are related to the structure of the final complex and also the presence of solvent molecules, in solid state by synthesizing a wide range of different nuclearity complexes but concentrating on hybrid organic-inorganic compounds with infinite CuI chains. These chains are of interest for their particular photoluminescent properties and their usage for conductive wires. A 1D-cordination polymer whose overall light emission is white at room temperature due to the concomitant presence of a high- energy and a low-energy emission band was synthesize and fully characterized. The reversible transformation of an infinite single CuI chain into an infinite double CuI chain by simply grinding or heating the reagents was also discovered and thoroughly investigated.

As part of his research project, Francesco Farinella has developed a solid understanding of the issues involved, acquiring a complete mastery of the experimental techniques, developed original solutions to problems that have gradually presented, showing excellent ability to organize his own work in coordination with laboratory colleagues.

Francesco Farinella has also spent a five month research stage at the School of Chemistry, University of Nottingham under the supervision of Prof. Neil

Champness. He has prepared and characterized a range of new coordination frameworks and developed a new type of ligand based on pyrogallol[4]arene. Major achievements in the three years' research are documented by two scientific articles published in major international journals, while other two papers are being prepared. He has also attended five national and international schools and conferences in which he presented both posters and oral communications, showing excellent knowledge and organizational capacity of the scientific material and effective communication skills. He also attended the school "1st Excelsus Advanced Lectures of X-Ray Crystallography" by Prof. Carmelo Giacovazzo.

In my opinion Francesco Farinella has carried out a very good work for the thesis.

1 Introduction

Complexes based on metals with d^{10} configuration (Cu, Ag, Au) are currently in the focus of numerous research studies because of the demand for materials active in optoelectronic devices.[1–7] The interest arises from the increasing demand of more-affordable complexes in preference to luminescent metal complexes based on precious and rare-earth metals, Ir, Pt or Os, which are often quite expensive and environmentally problematic[8], which complicates their usage in high-volume productions[9–11].

The copper iodide complexes present several advantages, because compared to the corresponding clusters with Br- and Cl- tend to be more stable in air and show a more intense luminescence in the solid state.[12,13] Most of the complexes studied are characterized by a remarkable high quantum yield in solid state[14–17], they are characterized by a large variety of coordination geometries[10,15,18,19] which arise from the many possible combinations of coordination numbers (two, three and four) available for copper(I) and geometries that can be adopted by the halide ions (from terminal to μ_2- and up to μ_8-bridging);[20,21] they present different excited states which can be of a ligand centered, charge transfer or, in the case of polynuclear compounds, even metal-centered nature;[12,22–24] and finally the reagents are cheap and the synthetic procedures are easy and occur in few steps.[7,10,20,25–27]

Copper iodide complexes can have a ^{3}XLCT emission band if we are in the presence of aromatic ligand and a ^{3}CC if the distances between the metal centers are shorter than the sum of the van der Waals radii, that in the case of Cu is 2.8 Å[28]. Furthermore due to the great differences in the geometries of CuI compounds, lots of different synthetic techniques, such as the solution methods, mechanochemical[20] (grinding and liquid assisted grinding), solvothermal, vapour or liquid diffusion, need to be used. All of these aspects will be treated in detail in the next chapters.

Photophysical properties of copper (I) complexes

Cuprous halide salt and organic bases usually form polynuclear complexes with general formula $Cu_nX_nL_m$ (X=Cl, Br or I; L = N- or P-bound ligand) that have been studied since the beginning of the 20th century. Copper (I) complexes are widely studied due to their unique structural and photophysical properties. These complexes present different luminescent states which can have different natures: ligand centred or, metal-centred especially in the case of polynuclear compounds,[22,12] and charge transfer. The luminescent aspects can vary with the temperature or the rigidity of the matrix in which the compounds are dispersed, and these aspects contribute to make copper iodide complexes very attractive for luminescence and structural studies. In the 70s Hardt and co-workers studied different CuI(pyridine) complexes[29]. In particular, ($CuIpy_3$) crystals didn't show any fluorescent behavior at room temperature but showed yellow fluorescence upon the increasing the temperature to 180°C. ($CuIpy_2$) instead showed a green fluorescence even at room temperature as well as at very low temperatures. (CuIpy) showed yellow fluorescence at room temperature which reversibly changed to orange, then to red and finally to violet by cooling in liquid nitrogen. To explain the strange behavior of these complexes upon changing the temperature he coined the term **luminescence thermochromism**. Later, in the 90s, Ford et al. continued a careful and extensive research project, both experimentally[22,30,31] and theoretically[23,24] focused on the luminescent properties of $Cu_4I_4py_4$ and its derivatives discovering that the change in color was due to two distinct emission bands. The first one, at high-energy, is attributed to halide-to-ligand charge transfer (^{3}XLCT) and is only possible in the presence of aromatic ligand because of the presence of excited state accessible to the electronic density from the halogen. The second one, at low-energy, attributed to a triplet Cu-I cluster-centered (^{3}CC) excited state, arises from a combination of halogen to copper charge transfer and d⟶s transitions, with the excitation localized in the copper-halogen core and thus, due to this reason, only possible in the presence of an interaction between the metal centers.

In the case of Cu(I) the metal-metal distance needs to be shorter than 2.8 Å[28] even if recently, the van der Waals' radius of Cu was revalued by 1.4 Å to 1.9 Å

thus shifting the limit value from 2.8 Å to 3.8 Å [32] Most of the studied complexes are characterized by a considerable high quantum yield in the solid state.[5,6,14] Recently, the possibility of the emission properties of copper (I) compounds have been enlarged. In 2011, Yersin and co-workers found that copper complexes are prone to present thermally activated delayed fluorescence (TADF)[33]. Several Cu(I) compounds with bidentate ligands (P^N) present a low singlet–triplet splitting ($\Delta E(S_1 - T_1) \approx 10^2$ cm^{-1}) which allows the so called singlet-harvesting effect and the emission from both the singlet and the triplet excited state depending on the temperature. The singlet excited state, which is slightly higher in energy than the triplet state, can be thermally activated at the expense of the triplet state. The TADF emission mechanism involves both singlet and triplet states, and therefore, it has been exploited for singlet and triplet excitons for the generation of light in an electroluminescent devices.[34]

Structural properties and experimental techniques

Copper halides complexes are involved in both kinetically fast dissociative and associative equilibria[35] and this make its study in solution particularly difficult, furthermore, the labile coordination numbers and geometries of both copper(I) and halide ions allow an inner-core variability difficult to predict *a priori*. These complexes are thus characterized by a wide energy landscape confirmed by the presence of several different copper halides complexes. Discrete dimers, cubane tetramers, stepped cubane tetramers, infinite polymeric chains (including split stairs, zig-zag, helical, staircase, rack and columnar ones) are part of the extremely various landscape of copper halides complexes present in the Crystallographic Structure Database[27] which show dramatically different nuclearity of the CuxIy cores. Although the final structures of the copper(I) halide complexes in crystals are arduous to design, the reaction stoichiometry allows some degree of control of the copper(I) halide core. It has been observed that the reactions with a stoichiometry ratio between the copper and the ligand higher than one (CuI/L >>1) promote a greater nuclearity while a stoichiometry ratio between the copper and the ligand lower than one (CuI/L <<1) promote the formation of monomers.[36] However, to explore all the possible crystal forms

it is necessary to change not only the stoichiometry but also other parameters such as solvent, temperature and synthetic procedures etc..

In the following chapter different experiments in which CuI has been reacted with different N^N and P^N-based ligands are reported. Organophosphine copper(I) halides have been extensively studied in the past and several species with different metal coordination numbers and metal to ligand ratios have already been reported.

The stoichiometry ratio between the reagents is only one of the parameters that can be modified to probe the geometry landscape of copper(I) complexes. In spite of the presence of plenty of complexes in solution, pure compounds can be obtained as powders: in fact while the stoichiometry ratio determines the nuclearity of the compounds, the polymorph or isomer outcome can be influenced by the choice of solvent (polar or a-polar, protic ecc) or by the procedure used. The CuI has a low solubility in most of the common solvents (only soluble in a saturated aqueous solution of KI or acetonitrile) which restricts the possibility of changing the solvent. To overcome the problem of the low solubility the reactions can be performed in solid state which can yield crystal forms hardly or even not obtainable with conventional methods.[20,37] The reactivity of nitrogen, sulphur or phosphorous based ligands towards CuI is very high and many works of mechanochemical synthesis are reported[38,39] which led to the formation of compounds not obtainable by solution synthesis. The main drawback in the solid state reaction methods (ball milling, grinding) consists in the formation of microcrystalline products, not suitable for X-ray single crystal diffraction. Due to the great reactivity of the aromatic ligands, previously cited, with CuI it often results difficult to obtain crystals suitable for SCXR diffraction and most of the time traditional crystallizations from solution, but also triple layer crystallizations, or seeding of solutions with microcrystalline powder of the desired compound fail to yield single crystals of suitable size for single crystal diffraction experiments. However, the structure can be determined from X-ray powder diffraction data, thanks to the development of "direct space" methods.[40] Structure solution from powder diffraction data has thus developed rapidly over the past ten years and powder

diffraction itself has played a central role in structural chemistry, physics and material sciences.

Structure determination from X-ray powder diffraction data

The structural characterization represents a key point to understand the properties and to design new compounds.

There are several advantages in structural studies of materials. The characterization of high temperature superconductors, materials for molecular hydrogen storage, luminescent materials, has relied heavily on powder diffraction techniques. Nowadays solving the 3D-structure of a molecular material by performing a single crystal X-ray diffraction analysis is relatively easy. However, having at least a single crystal suitable in dimensions and purity is a key point for this analysis which still remains the bottleneck step and, in the worst case, even if a single crystal has been obtained, the structure of the material might not correspond to that of the bulk powder.[1] The developments of powder diffraction have been thus driven by a growing need for tools that are able to probe the structures of materials that are only available in powder form, or can only be studied as powders. In these unlucky cases, structure solution from powder data seems to be the only way to reach the correct crystalline structure, even if the steps for the structure determination from powders are not yet as routine as it is with single crystal diffraction. The main reason why the structure determination from powder diffraction data is much more complex than from single crystal data is associated almost entirely with the collapse of the 3D crystallographic information onto the 1D powder pattern.[2] The structure determination process can be very difficult and not straightforward and sometimes the best way to reach the solution could be neither the shortest nor the simplest one. Although there are many paths that can followed in the quest for the exact structure, they are not all appropriate or even practicable for a given problem and the user experience plays a key role to finally solve the structure. The two main points for the structure solution from powder diffraction data are the following: (i) determination of the unit cell and space group and (ii) structure solution via the simulated annealing method

starting from the molecular building units. The goodness of the unit cell found can be verified from the figure of merit (FOM), the higher the better, and the comparison of the cell volume with the molecular volume. Most of the time in the case of CuI complexes the molecular volume is not known, since the CuI : ligand stoichiometry ratio in the structure cannot be assumed from the synthesis. The cells with the best FOM are used to guess the stoichiometry ratio and the result are compared with the TGA curves. The weight losses before 300 °C, in the Thermogravimetric Analysis, are usually assigned to the release of the ligand and the release of solvent molecules, if present. The simulated annealing algorithm is usually performed with the copper and the iodide atoms unbound and the ligand described as a rigid body. Other spectroscopy techniques like IR or Solid State NMR can give some insights on the coordination or on the asymmetric units but not assure the solution.[41,42]

Determining the crystalline structure from powder diffraction data gives the possibility to overcome the lack of suitable single crystals for SCXRD. The grade of success will depend upon the quality of the data and these, in turn, depend in quality of the sample. So, to improve the sample purity and crystallinity and then the data collection is performed as best as possible increasing the exposition time and reducing the step size. Working with lab data (and with kα1 and kα2 Cu radiation source) makes the indexing step more complicated than it actually is and the determination of the correct lattice parameters comes out from several considerations. The golden rule is that the lattice volume should be coherent with the stoichiometry previously found and then, it is a good practice to use different indexing algorithms: if they give the same lattice parameters, it could be a signal that it is the right path. The quest of suitable methods to obtain crystals for structure determination of copper complexes led us to explore different crystallization processes including those based on solvothermal synthesis. Recently**,** several zeolites which are commonly obtained by solvothermal synthesis, have been reproduced by grinding or ball milling,[43–46] which suggests that the solid state reactions can have several aspects in common with the solvothermal conditions.[47] The latter method consist of the increase of the temperature and consequently of the pressure inside a teflon-lined steel autoclave while the mechanochemistry via ball milling consist of a

fast movement of the balls within the jars that produce a localized increase of the pressure in the hit point with a consequently increase of the temperature. Nowadays for large scale preparations, researches are trying to move from solvothermal to solvent–free reactions in order to reduce environmental impact and energy consumption. Solvothermal synthesis can still be exploited to obtain single crystals of the desired compound since the high-temperature and high-pressure environment conditions created, would facilitate the crystallization process of complexes with poor solubility.

Structure-property relationship

The structure-properties relationship is the key point to design new compounds with tailor made properties. In this sense, systematic researches have been presented to better understand or to verify the role of both the ligand nature and the core.

In 2013 Volz et al. presented a work that described the possibility of tuning both luminescence and solubility of dimeric CuI complexes by acting on the opportune site. The ancillary ligands are mainly responsible of the solubility[10] and do not affect the emission profile while the bridging ligand[15] is, indeed, responsible for the luminescence. Theoretical studies have, in fact, demonstrated that the HOMO/LUMO orbitals are concentrated on the copper iodide core and the bridging ligand respectively. Electron-rich ligands (imidazole, benzimidazol, triazol) can shift the emission color towards the blue region, while the electron-poor ligands towards the red region. The possibility of tuning the solubility opens a wide landscape of solution processing techniques required for the deposition of the emissive layer on the devices.

As already discussed, the wavelength emission profile is also function of the metallophilic interaction due to copper-copper distances lower than the sum of van der Walls radii for the ^{3}CC emission band or the aromatic nature of the ligand for the ^{3}XLCT emission band. The quantum yield emission is an important parameter to be considered as much as the wavelength emission.

However, the photophysical properties of the solids could be very different from those in solution: first of all because most of the complexes are insoluble in the

common solvents, second due to kinetically fast dissociative and associative equilibria that may undergo some compounds and third the molecular organization through the crystals, which can be expected to affect the energies and/or the kinetics of the excited states. [38,39,48]

In this respect, polymorphism (the existence of different crystal forms for the same molecular or supramolecular entity), could play a key role in determining the final photophysical properties.[36]

Single phase white-emitting compounds

White organic light-emitting diode (WOLED) technology is a particular branch of OLED research due to its merits of high resolution and flexible possibility for large-scale production of solid-state light sources displays and full-color OLEDs.[49–51] Generally, white light can be obtained by using red (R), green (G), and blue (B) triple-doped emitters in a single layer. However, this triple dopant (R–G–B) strategy can be problematic due to the inter dopant energy transfer, leading to an imbalance in the white color.[52] Triple-emission-layer WOLEDs are also popular for their better balanced white light obtained[53] but the problems of undesired chromaticity as well as poor batch-to-batch reproducibility would result in low image-quality displays[54].

From the invention of the first light bulbs, to the implementation of fluorescent tubes, up to the presently fast-growing solid-state lightening, it has been the key fixture in defining the quality of modern life. In a WOLED, white light is typically generated through the simultaneous emission of multiple emissive materials, which need to be employed in either a single emissive layer with multiple molecular emitters or multiple emissive layers.[55] One of the current academic interests is in the quest for single white light phosphors to avoid the intrinsic colour balance, device complication, and high-cost problems when using multiphosphors or multi-LEDs.[56] Examples are rare but still can be found in the research field of organic molecules or polymers,[57–61] metal-doped or hybrid inorganic materials,[62–65] metal complexes,[66–68] and nanomaterials.[69–71] Here a single phase white emitter copper complex is proposed in which both ^{3}CC and ^{3}XLCT are contemporary present at room temperature. The two

emission bands are surprisingly complementary in an overall white emission at naked eye.

OLED device

Luminescent copper(I) complexes are described to be very good candidate for optoelectronics. Few examples are already reported in literature with good performance parameters[1,18,51,72] and it is plausible that the use of d^{10} complexes will increase in the next years as active material in luminescent devices. However, many problem still remain unsolved. The copper(I) complexes are generically not very soluble, which means that deposition processes such as drop casting or spin coating, which still remain the easiest way to deposit the emission layer, cannot be used in this case. Volz et al. eluded this problem with a series of extraordinary high efficient binuclear copper iodide complexes based on 2-pyridil-bisphophine ligand.[15,10] These kinds of complexes are soluble in organic solvents and are easily deposited via drop casting.

Collaboration project with CYNORA Gmbh

The purpose of this collaboration was to untangle the complicated luminescence properties of the sample called “cyUbo1” by a complete structure solution of the powder. A green luminescent whitish powder was obtained by synthesis in solution between CuI and the ligands (1,5-bis(diphenylphosphino)pentane) (L1)[82] and (2-diphenylphosphino-4-methylpyridine) (L2).[11] The photophysical properties resulted difficult to figure out because of the strange behaviour of the compound upon mechanical stresses. When grinded, the luminescence changed from intense green to deep orange and also the melting point changed between the “virgin” powder and the grinded one but there was no evidence of changes in the powder pattern. A recrystallization by slow diffusion of diethyl ether in a CH_2Cl_2 solution of the powder was thus performed that led to the formation of multiple crystals. From the batch of crystallization different crystal forms characterized by different emission light under UV radiation were isolated. It was possible to isolate crystals suitable for single crystal Xray diffraction for the phases: Cu_3I_3 (1,5-bis (diphenylphosphino)pentane)(2-diphenylphosphino-4-methylpyridine), Cu_2I_2(1,5-bis(diphenylphosphino)pentane)$_2$ and Cu_2I_2(2-diphenylphosphino-4-methylpyridine)$_3$.

Hybrid organic-inorganic materials

A great part of the research was focused on the synthesis and characterization of the so called “organic-inorganic hybrids”[73,74] based both on copper iodide and silver iodide because they present similar structural and photophysical properties. The organic-inorganic hybrid materials are of interest for the preparation of compounds with different characteristics thanks to the possibility of combining properties, such as high thermal and mechanical stability, high electrical conductivity, typical of inorganic compounds, with those typical of organic systems, such as structural flexibility and low cost[56,75,76].

The term organic-inorganic hybrids defines those materials that consist of an organic moiety and of an inorganic fraction, where the metal-ligand connectivity is interrupted by "inorganic" bridges. Despite the great success, the utilization of hybrid materials has been so far mainly based on the nature of the inorganic components while the role of the organic one is confined to supporting the inorganic architecture[77]. These utilizations can vary from the manufacture of light-emitting devices to that of electrical conduction[78]. A subgroup of hybrids, is represented by those based on silver halides and nitrogen ligands, interesting for the diversity of structures in which they can be synthesized. Silver salts show an intense luminescence, especially at low temperature[79,80], in the solid state following almost the same behaviour of CuI salts. This phenomenon has proved to be particularly pronounced for crystal structures with short contacts between silver atoms, less than 3.44 Å[80] and it is referred to by the term "argentophilic interaction”.

The reaction mechanisms are similar to those used for copper(I) salts because of the extremely low solubility. The problem can be partially overcome by using a rich solution of I^- ions to favor the formation of the complex $[AgI_4]^{-}$[81].

References

1 Z. Liu, M. Qayyum, C. Wu, M. T. Whited, P. I. Djurovich, K. O. Hodgson, B. Hedman, E. I. Solomon and M. E. Thompson, *J. Am. Chem. Soc.*, 2011, **133**, 3700–3.

2 D. Volz, L. Bergmann, D. M. Zink, T. Baumann and S. Bräse, *SPIE Newsroom*, 2013, 2–4.

3 J. C. Deaton, S. C. Switalski, D. Y. Kondakov, R. H. Young, T. D. Pawlik, D. J. Giesen, S. B. Harkins, A. J. M. Miller, S. F. Mickenberg and J. C. Peters, *J. Am. Chem. Soc.*, 2010, **132**, 9499–9508.

4 Q. Zhang, T. Komino, S. Huang, S. Matsunami, K. Goushi and C. Adachi, *Adv. Funct. Mater.*, 2012, **22**, 2327–2336.

5 Z. Wu, J. Luo, N. Sun, L. Zhu, H. Sun, L. Yu, D. Yang, X. Qiao, J. Chen, C. Yang and D. Ma, *Adv. Funct. Mater.*, 2016, **26**, 3306–3313.

6 Z. Liu, J. Qiu, F. Wei, J. Wang, X. Liu, M. G. Helander, S. Rodney, Z. Wang, Z. Bian, Z. Lu, M. E. Thompson and C. Huang, *Chem. Mater.*, 2014, **26**, 2368–2373.

7 F. Farinella, L. Maini, P. P. Mazzeo, V. Fattori, F. Monti and D. Braga, *Dalt. Trans.*, 2016, **45**, 17939–17947.

8 T. Vander Hoogerstraete, S. Wellens, K. Verachtert and K. Binnemans, *Green Chem*, 2013, **15**, 919.

9 D. Volz, M. Nieger, J. Friedrichs, T. Baumann and S. Br??se, *Langmuir*, 2013, **29**, 3034–3044.

10 D. Volz, D. M. Zink, T. Bocksrocker, J. Friedrichs, M. Nieger, T. Baumann, U. Lemmer and S. Br??se, *Chem. Mater.*, 2013, **25**, 3414–3426.

11 S. Zink, D. M.; Bächle, M.; Baumann, T.; Nieger, M.; Kühn, M.; Wang. C.; Klopper, W.; Monkowius, U.; Hofbeck, T.; Yersin, H.; Bräse, *Inorg. Chem.*, 2012, **52**, 2292–2305.

12 P. C. Ford, E. Cariati and J. Bourassa, *Chem. Rev*, 1999, **99**, 3625–3647.

13 D. Volz, M. Nieger, J. Friedrichs, T. Baumann and S. Bräse, *Inorg. Chem. Commun.*, 2013, **37**, 106–109.

14 M. Wallesch, D. Volz, D. M. Zink, U. Schepers, M. Nieger, T. Baumann and S. Bräse, *Chemistry*, 2014, **20**, 6578–6590.

15 D. M. Zink, D. Volz, T. Baumann, M. Mydlak, H. Flügge, J. Friedrichs, M. Nieger and S. Bräse, *Chem. Mater.*, 2013, **25**, 4471–4486.

16 M. Wallesch, D. Volz, D. M. Zink, U. Schepers, M. Nieger, T. Baumann and S. Br??se, *Chemistry*, 2014, **20**, 6578–6590.

17 D. Volz, A. F. Hirschbiel, D. M. Zink, J. Friedrichs, M. Nieger, T. Baumann, S. Brase and C. Barner-Kowollik, *J. Mater. Chem. C*, 2014, **2**, 1457–1462.

18 D. M. Zink, D. Volz, T. Baumann, M. Mydlak, H. Flu, J. Friedrichs, M. Nieger and S. Bra, 2013.

19 Q. Benito, X. F. Le Goff, G. Nocton, A. Fargues, A. Garcia, A. Berhault, S. Kahlal, J. Y. Saillard, C. Martineau, J. Tr??bosc, T. Gacoin, J. P. Boilot and S. Perruchas, *Inorg. Chem.*, 2015, **54**, 4483–4494.

20 L. Maini, P. P. Mazzeo, F. Farinella, V. Fattori and D. Braga, *Faraday Discuss.*, 2014, **170**, 93–107.

21 R. Peng, M. Li and D. Li, *Coord. Chem. Rev.*, 2010, **254**, 1–18.

22 M. Vitale and P. C. Ford, 2001, **221**, 3–16.

23 M. Vitale, W. E. Paute and P. C. Ford, *J. Phys. Chem.*, 1992, 8329–8336.
24 F. De Angelis, S. Fantacci, A. Sgamellotti, E. Cariati, R. Ugo and P. C. Ford, *Inorg. Chem.*, 2006, **45**, 10576–10584.
25 X. Zhang, L. Song, M. Hong, H. Shi, K. Xu, Q. Lin, Y. Zhao, Y. Tian, J. Sun, K. Shu and W. Chai, *Polyhedron*, 2014, **81**, 687–694.
26 D. M. Zink, M. Bä, T. Baumann, M. Nieger, M. Kü, C. Wang, W. Klopper, U. Monkowius, T. Hofbeck, H. Yersin and S. Brä, .
27 P. Zhao, W. Jing, L. Jing, F. Jian and Y. Li, *Bull. Korean Chem. Soc.*, 2013, **34**, 3743–3748.
28 A. Bondi, *J. Phys. Chem.*, 1964, **68**, 441–451.
29 H. D. Hardt and A. Pierre, *Z. anorg. allg. Chem*, 1973, **402**, 107–112.
30 P. C. Ford and A. Vogler, *Acc. Chem. Res.*, 1993, **26**, 220–226.
31 P. C. Ford, *Coord. Chem. Rev.*, 1994, **132**, 129–140.
32 S. Batsanov, *Inorg. Mater.*, 2001, **37**, 871–885.
33 R. Czerwieniec, J. Yu and H. Yersin, *Inorg. Chem.*, 2011, **50**, 8293–8301.
34 M. J. Leitl, F. R. Küchle, H. A. Mayer, L. Wesemann and H. Yersin, *J. Phys. Chem. A*, 2013, **117**, 11823–11836.
35 C. H. Arnby, S. Jagner and I. Dance, *CrystEngComm*, 2004, **6**, 257–275.
36 L. Maini, D. Braga, P. P. Mazzeo and B. Ventura, *Dalt. Trans*, 2012, **41**, 531–539.
37 S. L. James, C. J. Adams, C. Bolm and D. Braga, *Chem. Soc. Rev.*, 2012, **41**, 413–447.
38 D. Braga, L. Maini, P. P. Mazzeo and B. Ventura, *Chem. - A Eur. J.*, 2010, **16**, 1553–1559.
39 D. Braga, F. Grepioni, L. Maini, P. P. Mazzeo and B. Ventura, *New J. Chem.*, 2011, **35**, 339–344.
40 W. I. F. David, K. Shankland, K. D. M. Harris, M. Tremayne, J. van de Streek, E. Pidcock, W. D. S. Motherwell and J. C. Cole, *Acta Crystallogr. A.*, 2006, **39**, 910–915.
41 G. A. Bowmaker, J. V Hanna, R. D. Hart, P. C. Healy, S. P. King, F. Marchetti, C. Pettinari, B. W. Skelton, A. Tabacaru and A. H. White, *Dalt. Trans.*, 2012, **41**, 7513–7525.
42 G. Bowmaker and J. Hanna, *… für Naturforschung. B, A J. …*, 2009, 1478–1486.
43 P. J. Beldon, L. Fábián, R. S. Stein, A. Thirumurugan, A. K. Cheetham and T. Friščić, *Angew. Chemie - Int. Ed.*, 2010, **49**, 9640–9643.
44 R. E. Morris and S. L. James, *Angew. Chemie - Int. Ed.*, 2013, **52**, 2163–2165.
45 Y. Jin, Q. Sun, G. Qi, C. Yang, J. Xu, F. Chen, X. Meng, F. Deng and F. S. Xiao, *Angew. Chemie - Int. Ed.*, 2013, **52**, 9172–9175.
46 J. F. Fern??ndez-Bertr??n, M. P. Hern??ndez, E. Reguera, H. Yee-Madeira, J. Rodriguez, A. Paneque and J. C. Llopiz, *J. Phys. Chem. Solids*, 2006, **67**, 1612–1617.
47 G. A. Bowmaker, *Chem Commun*, 2013, **49**, 334–348.
48 L. Maini, D. Braga, P. P. Mazzeo and B. Ventura, *Dalt. Trans*, 2012, **41**, 531–539.
49 L. Wang, D. W. Matson, E. Polikarpov, J. S. Swensen, C. C. Bonham, L. Cosimbescu, J. J. Berry, D. S. Ginley, D. J. Gaspar and A. B. Padmaperuma, *J. Appl. Phys.*, 2010, **107**.

50 B. W. D'Andrade and S. R. Forrest, *Adv. Mater.*, 2004, **16**, 1585–1595.
51 X. Niu, L. Ma, B. Yao, J. Ding, G. Tu, Z. Xie and L. Wang, *Appl. Phys. Lett.*, 2006, **89**, 1–4.
52 C. L. Ho, M. F. Lin, W. Y. Wong, W. K. Wong and C. H. Chen, *Appl. Phys. Lett.*, 2008, **92**.
53 R. J. Holmes, B. W. D'Andrade, S. R. Forrest, X. Ren, J. Li and M. E. Thompson, *Appl. Phys. Lett.*, 2003, **83**, 3818–3820.
54 C. L. Ho, W. Y. Wong, Q. Wang, D. Ma, L. Wang and Z. Lin, *Adv. Funct. Mater.*, 2008, **18**, 928–937.
55 G. M. Farinola and R. Ragni, *Chem. Soc. Rev.*, 2011, **40**, 3467–3482.
56 G.-E. Wang, G. Xu, M.-S. Wang, J. Sun, Z.-N. Xu, G.-C. Guo and J.-S. Huang, *J. Mater. Chem.*, 2012, **22**, 16742.
57 J. Y. Li, D. Liu, C. Ma, O. Lengyel, C. S. Lee, C. H. Tung and S. Lee, *Adv. Mater.*, 2004, **16**, 1538–1541.
58 M. Mazzeo, V. Vitale, F. Della Sala, M. Anni, G. Barbarella, L. Favaretto, G. Sotgiu, R. Cingolani and G. Gigli, *Adv. Mater.*, 2005, **17**, 34–39.
59 Y. Yang, M. Lowry, C. M. Schowalter, S. O. Fakayode, J. O. Escobedo, X. Xu, H. Zhang, T. J. Jensen, F. R. Fronczek, I. M. Warner and R. M. Strongin, *J. Am. Chem. Soc.*, 2006, **128**, 14081–14092.
60 J. Luo, X. Li, Q. Hou, J. Peng, W. Yang and Y. Cao, *Adv. Mater.*, 2007, **19**, 1113–1117.
61 J. Liu, Y. Cheng, Z. Xie, Y. Geng, L. Wang, X. Jing and F. Wang, *Adv. Mater.*, 2008, **20**, 1357–1362.
62 W. H. Green, *Science (80-.).*, 1997, **276**, 1826–1828.
63 T. Hayakawa, Y. Toh, M. Oshima, M. Matsuda, Y. Hatsukawa, N. Shinohara, H. Iimura, T. Shizuma, Y. H. Zhang, M. Sugawara and H. Kusakari, *Phys. Lett. Sect. B Nucl. Elem. Part. High-Energy Phys.*, 2003, **551**, 79–85.
64 L. Luo, X. X. Zhang, K. F. Li, K. W. Cheah, J. X. Shi, W. K. Wong and M. L. Gong, *Adv. Mater.*, 2004, **16**, 1664–1667.
65 Y. Liu, B. Lei and C. Shi, *Chem. Mater.*, 2005, **17**, 2108–2113.
66 G. Zhou, Q. Wang, C.-L. Ho, W.-Y. Wong, D. Ma and L. Wang, *Chem. Commun. (Camb).*, 2009, **2**, 3574–3576.
67 P. Coppo, M. Duati, V. N. Kozhevnikov, J. W. Hofstraat and L. De Cola, *Angew. Chemie - Int. Ed.*, 2005, **44**, 1806–1810.
68 R.-S. Liu, V. Drozd, N. Bagkar, C.-C. Shen, I. Baginskiy, C.-H. Chen and C. H. Tan, *J. Electrochem. Soc.*, 2008, **155**, P71.
69 H. S. Chen, S. J. J. Wang, C. J. Lo and J. Y. Chi, *Appl. Phys. Lett.*, 2005, **86**, 1–3.
70 X. M. Sui, C. L. Shao and Y. C. Liu, *Appl. Phys. Lett.*, 2005, **87**.
71 T. Uchino and T. Yamada, *Appl. Phys. Lett.*, 2004, **85**, 1164–1166.
72 M. J. Leitl, F. R. Küchle, H. A. Mayer, L. Wesemann and H. Yersin, *J. Phys. Chem. A*, 2013, **117**, 11823–11836.
73 E. Cariati, E. Lucenti, C. Botta, U. Giovanella, D. Marinotto and S. Righetto, *Coord. Chem. Rev.*, 2016, **306**, 566–614.
74 C. Janiak, *Dalt. Trans.*, 2003, 2781.
75 H. H. Li, Z. R. Chen, L. C. Cheng, M. Feng, H. D. Zheng and J. Q. Li, *Dalt. Trans*, 2009, 4888–4895.
76 A. Chen, S. Meng, J. Zhang and C. Zhang, *Inorg. Chem. Commun.*, 2013, **35**, 276–280.
77 S. Wang, D. B. Mitzi, C. A. Feild and A. Guloys, *J. Am. Chem. Soc.*, 1995, **117**,

5297–5302.
78 C. R. Kagan, D. B. Mitzi and C. D. Dimitrakopoulos, *Science*, 1999, **286**, 945–7.
79 J. Shen, C. Zhang, T. Yu, L. An and Y. Fu, *Cryst. Growth Des.*, 2014, **14**, 6337–6342.
80 H. Schmidbaur and A. Schier, *Angew. Chemie - Int. Ed.*, 2015, **54**, 746–784.
81 R. C. Zhang, Y. J. Zhang, B. Q. Yuan, J. P. Miao, B. H. Pei, P. P. Liu, J. J. Wang and D. J. Zhang, *J. Solid State Chem.*, 2014, **220**, 185–190.
82 (Di Nicola et al, Inorganica Chimica Acta 358 (2005) 763–795)

Chapter 1

MECHANOCHEMICAL PREPARATION OF COPPER IODIDE CLUSTERS OF INTEREST FOR LUMINESCENT DEVICES

Abstract: The copper iodide complexes are known for their large variety of coordination geometries. Such diversity, while making it difficult to predict the final structure, permits the preparation of a great number of copper iodide complexes based on the same ligand. The target of the research was that of thoroughly exploring the chemistry of CuI and the ligand diphenyl-2-pyridyl phosphine (PN) by varying the stoichiometric ratio and/or the aggregation state. Six different compounds have been identified: $[Cu_4I_4(PN)_2]$, $[Cu_4I_4(PN)_2{\cdot}(CH_2Cl_2)_{0.5}]$, $[CuI(PN)_{0.5}]_\infty$, $[CuI(PN)_3]$ whose structures have been determined during this study, $CuI(PN)_2$ which was characterized by powder diffraction and $[Cu_2I_2(PN)_3]$ which has been already reported. The preparation routes are also different: synthesis in solution yielded $[Cu_4I_4(PN)_2{\cdot}\ (CH_2Cl_2)_{0.5}]$ and $[CuI(PN)_3]$ while $[CuI(PN)_{0.5}]_\infty$ and $CuI(PN)_2$ were obtained only via solid state reactions. These two latter examples confirmed that mechanochemistry is a valid route to explore the landscape of the possible structures of CuI derivatives. Crystallization by traditional solution procedures failed to give the desired crystal, so structure determination of the new compounds was tackled in two ways: by attempting crystal growth via solvothermal synthesis and by resolving the structure from X-ray powder diffraction data with “direct space” methods. What is more the photophysical properties of the complexes that could be obtained as sufficiently pure powders have also been investigated and are reported herein.

Introduction

Complexes based on copper iodide are currently at the forefront of coordination chemistry and crystal engineering research because of the quest for active materials in optoelectronics.[1–8] The interest stems from the increasing demand of more-affordable complexes in preference to luminescent metal complexes based on precious (i.e. the platinum group) and rare-earth metals, which are often quite expensive and environmentally problematic.[9] The copper iodide complexes present several advantages: they are characterized by a large variety of coordination geometries which arise from the many possible combinations of coordination numbers (two, three and four) available for copper(I) and geometries that can be adopted by the halide ions (from terminal to μ_2- and up to μ_8-bridging);[10] they present different luminescent levels which can be of a ligand centred, charge transfer or, in the case of polynuclear compounds, even metal-centred nature;[11,12] most of the complexes studied are characterized by a remarkable high quantum yield in solid state;[4,13,14] and finally the reagents are cheap and it is relatively easy to obtain the final products.[4,15] The luminescent properties of copper(I) halide clusters are strictly related to the geometries adopted by the clusters.[12] In the case of the cubanes $Cu_4I_4L_4$ for example, two distinct emission bands were observed, the high-energy band attributed to halide-to-ligand charge transfer (^{3}XLCT), and the low-energy emission band was attributed to a triplet Cu-I Cluster-Centered (^{3}CC) excited state with the excitation localized to the Cu_4I_4 core, only possible in the presence of an interaction between the metal centres. Recent studies have widened the possibility of the emission properties of copper(I) compounds. Several Cu(I) compounds with P^N ligands present a low singlet–triplet splitting which allows the emission from both the singlet and the triplet excited state depending on the temperature. The singlet excited state, which is slightly higher in energy than the triplet state, can be activated thermally at the expense of the triplet state, leading to the so-called thermally activated delayed fluorescence (TADF). The TADF emission mechanism allows harvesting of both singlet and triplet excited states generated by charge recombination in electroluminescent devices, therefore light generation efficiency is enhanced.[13,16] Due to the increasing interest in CuI(P^N ligands) complexes for OLED applications and for

photochemistry studies,[3,13,15,17] we exploited the reactivity of the CuI towards diphenyl-2-pyridyl phosphine, hereafter PN. Two crucial aspects of the research will be presented: we will first discuss how the synthetic procedure influences the formation of the final product with particular attention to the mechanochemical synthesis; secondly we will address the different strategies to determine the crystal structure when the final product is a crystalline powder. The crystal engineering of copper halides is particularly difficult since in solution, halocuprate complexes are involved in kinetically fast dissociative and associative equilibria[18,19] and the labile coordination numbers and geometries of both copper(I) and halide ions allows an inner-core variability difficult to predict. These complexes are characterized by a flat energy landscape confirmed by the presence of several different copper halides complexes in the CSD[20] which present dramatically different nuclearity of their CuxIy cores such as discrete dimers, cubane tetramers and stepped cubane tetramers to infinite polymeric chains (including split stairs, zigzag, helical, staircase, rack and columnar structures). Although the final structures of the copper(I) halide complexes in crystals could be hardly designed, the reaction stoichiometry allows some degree of control of the copper(I) halide core: reactions with a stoichiometry ratio of CuI/L>>1 higher nuclearity are favored while CuI/L << 1 promote the formation of monomers.[21] However, to explore all the possible crystal forms it is necessary to vary not only the stoichiometry but also other parameters such as solvent, temperature etc. To overcome the problem of the low solubility of the CuI which restricts the possibility of changing the solvent, the reactions can be performed in the solid state which can yield crystal forms hardly or even not obtainable in solution.[22] The reactivity of CuI towards nitrogen, sulphur or phosphorus based ligands is very high and preliminary work on mechanochemical synthesis with CuI with N-based satured ligands has been reported;[23,24] more extensive studies have been done for copper thyocyanate complexs,[25–27] in both cases mechanochemical synthesis led to the formation of compounds not obtained by solution synthesis. The main drawbacks in the mechanochemical reaction methods consist of the formation of microcrystalline products, obviously unsuitable for X-ray single crystal diffraction. Structural characterization is a key point to under- stand the

properties of the compounds and to design new compounds, which is why great effort will be devoted to tackling this problem. Most of the time traditional crystallization from solution, but also triple layer crystallizations or seeding of solutions with microcrystalline powder of the desired compound, fail to yield single crystals of amenable size for single crystal diffraction experiments. However, the structure can be determined from X-ray powder diffraction data, thanks to the development of "direct space" methods.[28] This approach is particularly suited for materials constructed from well-defined modular building units and it is more challenging for copper iodide complexes whose coordination is difficult to control. Spectroscopy techniques such as IR or Solid State NMR can give some insights on the coordination or on the asymmetric units but not guarantee exact structure determination.[26,29] The quest of suitable methods to obtain crystals for structure determination of copper complexes led me to explore different crystallization processes, including those based on solvothermal synthesis. Recently, several zeolites, commonly obtained by solvothermal synthesis, have been produced also by grinding or ball milling,[30–33] which suggests that the solid state reactions can have several aspects in common with solvothermal conditions.[25] Although, for large scale preparations, nowadays researchers try to move from solvothermal to solvent-free reactions in order to reduce their environmental impact and energy consumption, solvothermal synthesis can still be exploited to obtain single crystals of the desired compounds since the high-temperature and high-pressure environments conditions created would facilitate the crystallization process of complexes with poor solubility. Herein we report the synthesis of five new crystal forms of copper iodide with the diphenyl-2-pyridyl phosphine (PN): $[Cu_4I_4(PN)_2]$, $[Cu_4I_4(PN)2{\cdot}(CH_2Cl_2)_{0.5}]$, $[CuI(PN)_{0.5}]_\infty$, $[CuI(PN)_3]$ and $CuI(PN)_2$; as well as that of the known complex $[Cu_2I_2(PN)_3]$.[14] Mechanochemical synthesis was decisive to obtain the new compounds $[CuI(PN)_{0.5}]_\infty$ and $CuI(PN)_2$ while the monomer $[CuI(PN)_3]$ is formed only by precipitation from solution. Not only the stoichiometry variation but also performing the reaction in solid state or solution allowed me to widen the land- scape of the crystal forms of copper iodide complexes with PN. The structures of $[Cu_4I_4(PN)_2]$ and $[CuI(PN)_{0.5}]_\infty$have been determined by single crystals obtained from solvothermal synthesis, while

the bulk product has been obtained by reaction in solid state or solution. The structure of $[CuI(PN)_3]$ was determined by direct methods from X-ray powder diffraction data. All the compounds obtained are luminescent and the photophysical properties of the complexes that could be obtained as sufficiently pure powders, have been studied and reported.

Experimental part

General

All reagents were purchased from Sigma Aldrich and used without further purification.

Synthesis of $[Cu_2I_2(PN)_3]$

Copper(I) iodide (0.380 g; 2 mmol) and the PN ligand (0.789 g; 3 mmol) were suspended under nitrogen atmosphere in dry dichloromethane (10 mL) and stirred for 12 h at room temperature. The yellowish powder obtained was filtered and washed with a saturated solution of KI aq to remove the unreacted CuI and distilled water to remove KI. The title compound was obtained by grinding CuI (0.190 g; 1 mmol) and PN (0.394 g; 1.5 mmol) with two drops of acetonitrile in a ball mill for 30 minutes at 20 Hz.

Synthesis of $[CuI(PN)_3]$

Copper iodide (0.095 g, 0.5 mmol) was dissolved in saturated aqueous solution of KI (5 mL) then an acetone solution of PN (0.526 g, 2 mmol) was added under stirring. A whitish powder precipitates instantly which was filtered and washed with cold acetone.

Synthesis of $CuI(PN)_2$

Copper iodide (0.190 g; 1mmol) and PN ligand (1.052 g; 4 mmol) were ground with two drops of AcCN in a ball mill for 60 minutes at 20 Hz.

Crystallization of $[Cu_4I_4(PN)_2]$ and $[CuI(PN)_{0.5}]_\infty$

Crystals of $[Cu_4I_4(PN)_2]$ suitable for SC-XRD analysis were obtained in a 5 mL reactor via solvothermal synthesis by mixing 0.2 g of CuI with 0.8 g of PN in 1 mL of ethanol at 170 °C and slowly cooling down to ambient temperature over 7 days. Crystals of $[CuI(PN)_{0.5}]_\infty$ suitable for SC-XRD were obtained in a 5 mL reactor via solvothermal conditions by mixing 0.2 g of CuI with 0.6 g of PN in 1 mL of toluene at 140 °C and slowly cooling down to ambient temperature over 7 days.

TGA measurements

TGA measurements were performed using a Perkin Elmer TGA7 in the temperature range 35–700 °C under N_2 gas flow and heating was carried out at 5 °C min^{-1}.

Photophysics

All determinations made use of powder samples placed between two quartz slides and were done at room temperature. Excitation and emission spectra were obtained with a SPEX Fluorolog fluorometer; excitation spectra were monitored at the maximum emission wavelength and emission spectra were recorded exciting all samples at 350 nm.

X-Ray powder diffraction

X-Ray powder diffractograms were collected on a Panalytical X'Pert PRO automated diffractometer with Cu Ka radiation and an X'Celerator equipped with an Anton Paar TTK 450 low-temperature camera. The program Mercury[34] was used for calculation of X-ray powder patterns. XRPD data of $[CuI(PN)_3]$ were collected over the range 3–70° 2θ with a Bruker D8 Advance diffractometer equipped with a LynxEye detector and focusing mirror.

Crystal structure determination

Crystal data for $[Cu_4I_4(PN)_2]$ and $[CuI(PN)_{0.5}]_\infty$ were collected on an Oxford Xcalibur S with MoKa radiation, λ=0.71073, monochromator graphite. Crystal data and details of measurements are summarized in Table 1. SHELX97[35] was used for the structure solution and refinement based on F2. Non-hydrogen atoms were refined anisotropically. The uniqueness of the crystal of $[CuI(PN)_{0.5}]_\infty$, synthesized by solvothermal reaction, did not allow the collection of better data. The bad quality data due to the poor crystallinity and high mosaicity of the sample. The Mercury[34] software package was used for the graphical representation of the resultant structures.

Results and discussion

Synthesis and crystal structures

The copper iodide was reacted with PN with different synthetic procedures which differed mainly in stoichiometric ratio or aggregation state (solid state or solution). The reactions in solution are carried out mainly in acetonitrile or a saturated aqueous solution of KI in air, while the reactions in the solid state were carried out via ball milling with a drop of acetonitrile or dichloromethane. Six different compounds have been isolated so far, $[Cu_2I_2(PN)_3]$ recently described by Zink et al.[13] $[Cu_4I_4(PN)_2]$ and its solvate form$[Cu_4I_4(PN)_2{\cdot}(CH_2Cl_2)_{0.5}]$, $[CuI(PN)_{0.5}]_\infty$, $[CuI(PN)_3]$ (whose structure has been determined during these studies) and $CuI(PN)_2$.

Table 1 Crystal data

	$[Cu_4I_4(PN)_2]$	$[CuI(PN)_{0.5}]_{\infty}$	$[CuI(PN)_3]$[a]
Chemical formula	$C_{34}H_{28}Cu_4I_4N_2P_2$	$C_{17}H_{14}Cu_2I_2N_1P_1$	$C_{51}H_{42}Cu_1I_1N_3P_3$
Formula Mass	1288.28	644.15	980.28
Crystal System	Monoclinic	Triclinic	Trigonal
a/Å	16.7222(3)	7.9805(7)	13.6471(2)
b/Å	13.9164(3)	8.5298(8)	13.6471(2)
c/Å	16.4466(3)	14.3667(14)	14.7400(4)
α/°	90	78.092(8)	90
β/°	99.688(2)	85.576(8)	90
γ/°	90	86.494(7)	120
Volume/ Å^3	3772.75(13)	953.05(15)	2377.4
Temperature	RT	RT	RT
Space group	$P2_1/c$	P-1	P-3
No. of independent reflections	11078	2594	-
R_{int}	0.0534	0.046	-
Final R_1 values	0.0489	0.1225	
Final $wR(F^2)$ values	0.0933	0.3395	
Final R_1 values (all data)	0.0621	0.1386	

[a] Solved from X-ray powder diffraction.

Table 2 Copper-copper distances

Compound		Distance/ Å
$[Cu_2I_2(PN)_3]$	Cu1-Cu2	2.7694(6)
$[CuI(PN)_{0.5}]_{\infty}$	Cu6-Cu7	2.7499(9)
	Cu5-Cu7	2.5883(9)
	Cu6-Cu8	2.574(1)
	Cu5-Cu8	2.699(1)
$[Cu_4I_4(PN)_2]$	Cu3-Cu4	2.771(7)
	Cu3-Cu3	2.900(7)
	Cu4-Cu4	3.485(6)

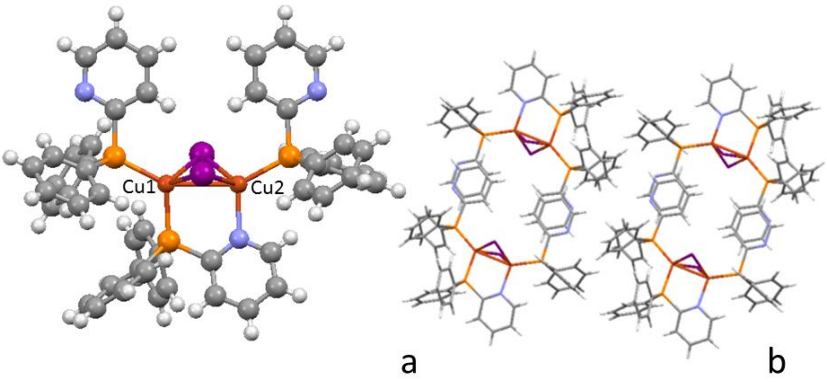

Fig.1 a) $[Cu_2I_2(PN)_3]$ b) π-π interactions present in the crystal packing

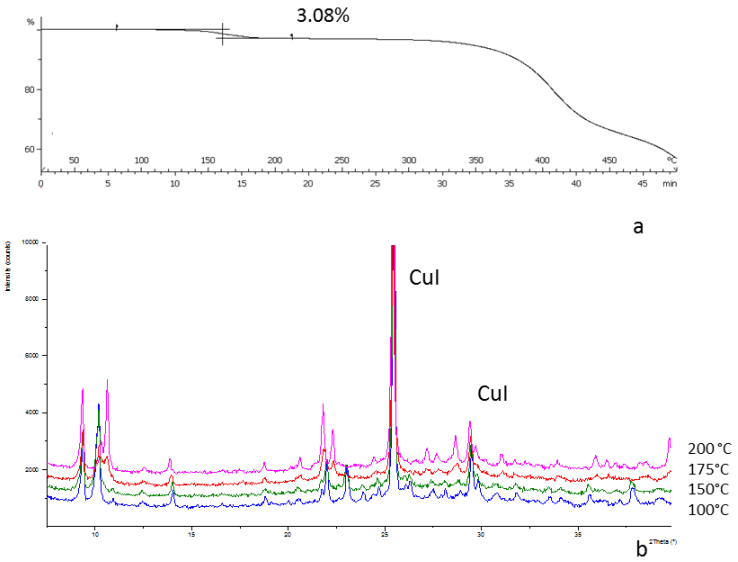

Fig. 2 a) TGA curve of $[Cu_4I_4(PN)_2{\cdot}(CH_3CN)]$, the first step is consistent with the release of one acetonitrile molecule (experimental 3.06%, calculated 2.96%), b) Variable temperature X-ray powder diffraction: pattern reported are at 100°C blue line, 150°C green line, 175°C red line and 200°C magenta line. Bragg reflections of unreacted CuI are highlighted with the label.

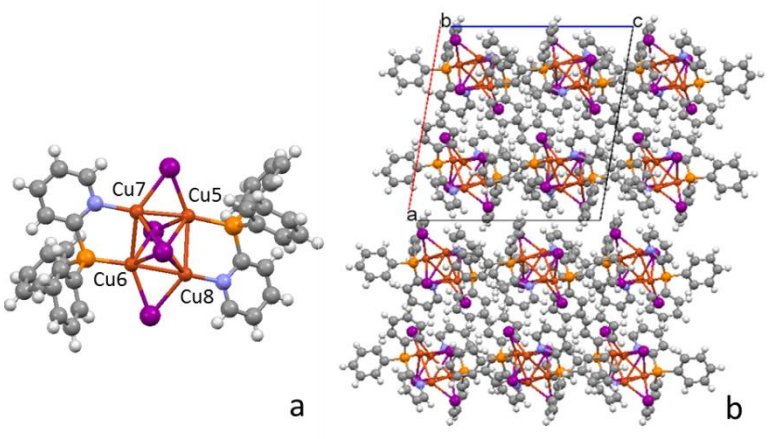

Fig.3 a) Compound $Cu_4I_4(PN)_2$; b) crystal packing view along *b axis*.

The dimer $[Cu_2I_2(PN)_3]$ was easily reproduced by the synthesis described in the literature13 and it was also obtained by ball milling of CuI and PN with a stoichiometry ratio 1 : 1.5 with a drop of acetonitrile. This complex seems to be very stable and it was obtained as an undesired product in several other reactions (up to a stoichiometry ratio CuI–PN 3 : 1 or 1 : 3) both in solution and the solid state.

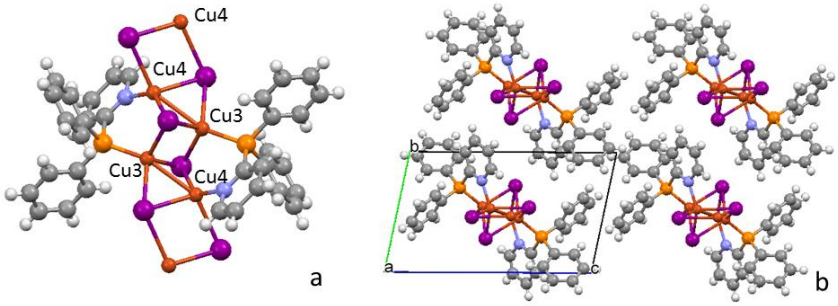

Fig. 4 a) Polymeric structure of $[CuI(PN)_{0.5}]_\infty$; b) crystal packing view along *a axis.* Polymeric chains run parallel to each other.

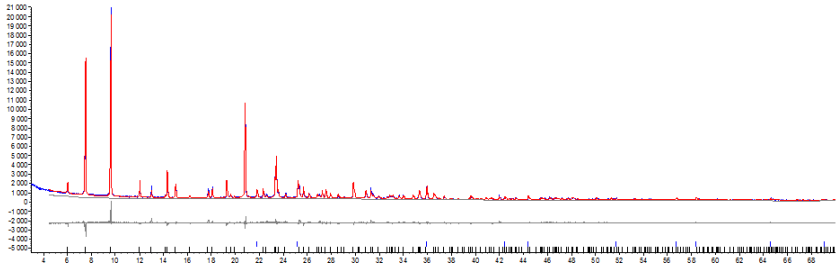

Fig. 5 Rietveld refinement of $[CuI(PN)_3]$, red line is the calculated diffractogram, blue line observed diffractogram and grey line difference plot. Blue ticks correspond to the Bragg peaks of KI, black ticks correspond to the Bragg peaks of $[CuI(PN)_3]$.

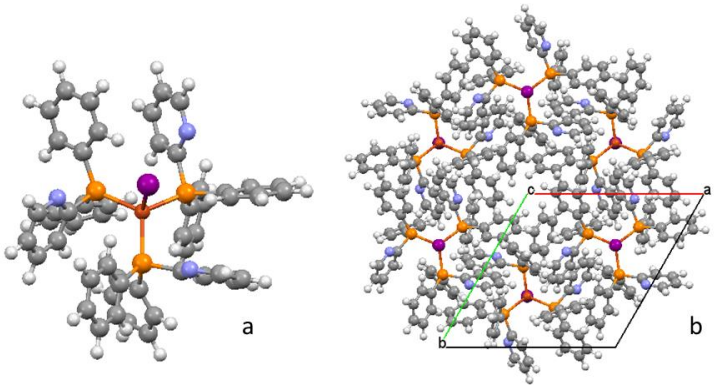

Fig.6 a) Single molecule of [$CuIPN_3$]; b) Packing of [$CuIPN_3$] view along the *c axis.*

In many cases in order to avoid the presence of [$Cu_2I_2(PN)_3$] the reactions were run with a great excess of one of the reagents. The dimeric core of [$Cu_2I_2(PN)_3$] is characterized by a butterfly shape due to the presence of a bridging ligand coordinating with both N and P atoms, and a short copper–copper distance (2.7694(6) Å) consistent with metallophilic interactions (see Table 2). The two other ligands coordinated only with the P atoms and they

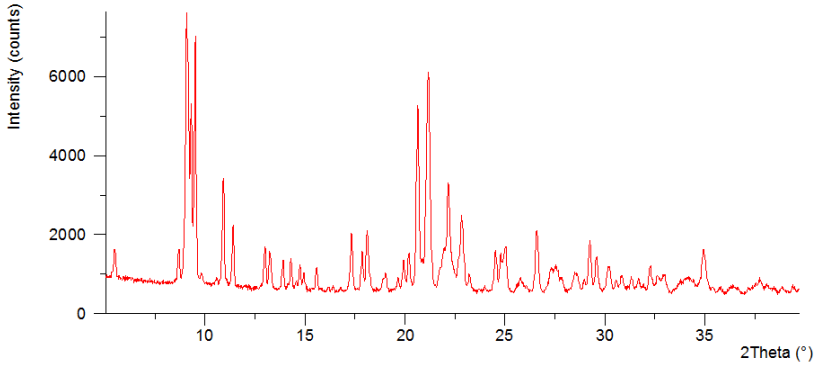

Fig. 7 Powder pattern of $CuI(PN)_2$ obtained by ball milling.

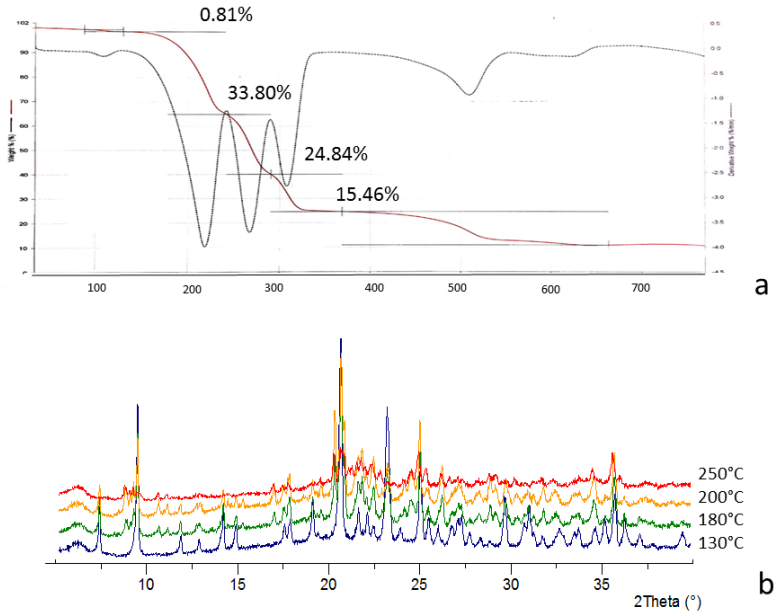

Fig. 8 a) TGA curve of $[CuI(PN)_3]$, the first step (0.81%) is due to some solvent release, the second step can be ascribed to the release to one ligand molecule (33.80%) which is suddenly followed by the release of the other ligand molecules; b) VTXRPD of $[CuI(PN)_3]$, at 180°C (green line) the peaks of $CuI(PN)_2$ appear, the complete transformation is characterized is observed at 250°C. The powder pattern presents a low crystallinity profile.

are described as ancillary ligands. The complexes interact via C–H––π and in the case of the ancillary ligands also via p–p interactions (see Fig. 1). These weak interactions do not affect the photophysical properties since the compound does not suffer emission quenching. The reactions carried in excess of CuI (stoichiometry ratio CuI–PN 4 : 1) lead to

the formation of $[Cu_4I_4(PN)_2{\cdot}(CH_2Cl_2)_{0.5}]$, and $[CuI(PN)_{0.5}]_\infty$; the pure phase of $[[Cu_4I_4(PN)_2{\cdot}(CH_2Cl_2)_{0.5}]$, is obtained by reaction in solution, while by ball milling a mixture of $[Cu_4I_4(PN)_2{\cdot}(CH_2Cl_2)_{0.5}]$and $[CuI(PN)_{0.5}]_\infty$ is obtained; it was not possible to isolate the pure phase of $[CuI(PN)_{0.5}]_\infty$. Single crystals of $[Cu_4I_4(PN)_2]$ and $[CuI(PN)_{0.5}]_\infty$ have been obtained by solvothermal reactions while all other attempts to obtain crystals by triple layer crystallization failed. $[Cu_4I_4(PN)_2{\cdot}(CH_2Cl_2)_{0.5}]$ presents a powder diffraction pattern very similar to $[Cu_4I_4(PN)_2]$; while the structure of the unsolvated form was determined by single crystal X-ray diffraction, it was only possible to index the powder pattern of the $[Cu_4I_4(PN)_2{\cdot}(CH_2Cl_2)_{0.5}]$.

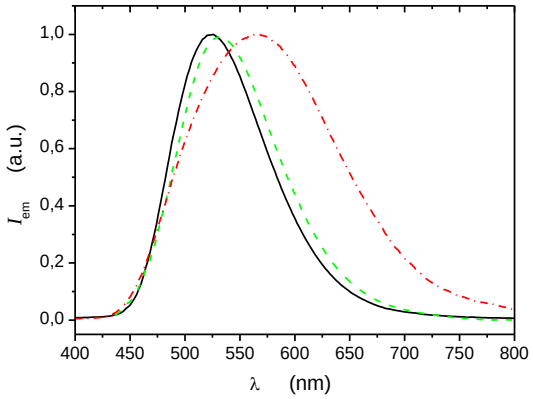

Fig. 9 Emission spectra of $[Cu_2I_2(PN)_3]$ (solid, black), $[CuI(PN)_3]$ (dash, green) and $[Cu_4I_4(PN)_2{\cdot}(CH_3CN)]$ (dash-dot, red) as crystalline powders at room temperature.

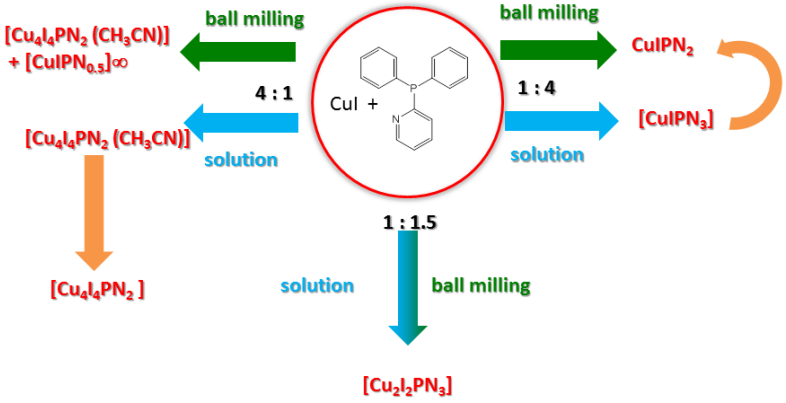

Scheme 1 Scheme of the compounds obtained and their relationship. Blue arrows indicate synthesis in solution, green arrows synthesis in solid state and orange arrows thermal treatment.

The Pawley refinement converged to Rwp = 6.65% with a monoclinic cell, space group $P2_1/c$ with parameters a=17.4853(5) Å, b=14.180(2) Å, c = 16.303(2) Å, β = 97.07(1)° and volume 4011.5(8) Å^3 which is about 239 Å^3 greater than the volume of $[Cu_4I_4(PN)_2]$. The difference in volume can be ascribed to the presence of dichloromethane molecules in the elementary cell. The presence of the solvent was confirmed by the TGA which shows a 3.08% weight loss at 150 °C corresponding to the release of half a molecule of dichloromethane (calculated 3.20%) (see Fig. 2a). The transformation of $[Cu_4I_4(PN)_2{\cdot}(CH_2Cl_2)_{0.5}]$ into $[Cu_4I_4(PN)_2]$ was observed also with variable temperature X-ray diffraction (see Fig. 2b). Instead of the common motif of cubane-like clusters, the $[Cu_4I_4(PN)_2]$ cluster adopts an "octahedral" geometry which has been observed recently by Liu et al.[4] The copper atoms are arranged in a parallelogram with μ^4-

iodides above and below the parallelogram and μ^2-iodides bridging the copper atoms on the short edge. All Cu–Cu distances are lower than the sum of the van der Waals radii (see Table 2). The aromatic ring interacts mainly via C–H----π interactions and π–π interactions involving the pyridine coordinating ring and a phenyl ring (see Fig. 3). The crystal packing suggests that the solvent molecules can be placed in the (1 0 0) plane, which is less dense. Further studies will be done to ascertain the crystal packing of $[Cu_4I_4(PN)_2{\cdot}(CH_2Cl_2)_{0.5}]$. It is worth noting that $[CuI(PN)_{0.5}]_\infty$ is easily obtained by mechanosynthesis, although not as a pure phase. Its formation was observed also in solid state reactions with a stoichiometry ratio CuI–PN 1 : 1.5. The low solubility of the compound, which characterizes all the coordination polymers, seems to preclude its formation from synthesis in solution, while it seems to be a driving force in the solid state reactions. The solvothermal conditions (high temperature and high pressure) allow the crystallization of phases which are known to be poorly soluble; in addition, solid state reactions are known to reach phases which can be hard to obtain in solution, as observed for the co-crystals.[36] In my case the solvothermal syntheses were explored in order to obtain a single crystal of the desired phase, since structure determination by X-ray powder diffraction (XRPD) would be very challenging due to the lack of information on the molecular geometry of the complexes. Despite of all the structures of CuI(P^N ligands) described in the literature[1–4,13,15,37] which show discrete complexes, the structure of $[CuI(PN)_{0.5}]_\infty$ is characterized by a one-dimensional copper iodide polymeric structure (see Fig. 4). The infinite double chain of CuI presents an alternation of short and long copper– copper distances (see Table 2). Usually the tetrahedral coordination of the copper(I) ions is fulfilled by multidentate bridging ligands to construct a 2D sheet network;[24,38] in our case the PN ligand bridges two copper atoms but on the same chain and brings the two copper atoms to a separation of 3.0716(3)˚ The reactions carried in excess of ligand leads to the formation of two new phases: $[CuI(PN)_3]$ and $CuI(PN)_2$. The pure compound $[CuI(PN)_3]$ is obtained only from reaction in solution carried out with a stoichiometry ratio of CuI–PN 1:4, but when the same reaction is carried out in the solid state only $CuI(PN)_2$ is obtained. The structure of $[CuI(PN)_3]$ was solved from powder pattern X-ray diffraction data even if the diffractogram acquired shows peaks of

unwashed KI salt. The powder pattern is indexed by a trigonal cell with cell axes a = 13.6471(2) Å, c = 14.7400(4) Å volume =2377 Å^3 and space group P-3. The volume of the asymmetric unit, 396 Å^3, is consistent with the volume of one third of [CuI(PN)$_3$]. This solution is possible only if the monomer is located on the 3-fold axis. The structure was solved with a simulated annealing algorithm using as starting model one molecule of the ligand not bonded to the metal atom and the copper atom and the iodide with a site occupancy of 1/3. The Rietveld refinement converged to Rwp = 7.681% and Rexp = 4.351% (see Fig. 5). The position of the nitrogen atoms was assumed from the structure solution since the packing features or the Rietveld refinement gave no hints on the possible position (see Fig. 6). The crystal packing of [CuI(PN)$_3$] does not present important intermolecular interactions. It is worth noting that along the c axis the molecular disposition creates cavities which can host solvent molecules as suggested also by the TGA curve (see Fig. 8a). Several attempts have been made to determine the crystal structure of CuI(PN)$_2$, although as the diffractogram does not present peaks of the reagents or of other known phases I was not able to index it (see Fig. 7). It is not possible to exclude the presence of more than one phase. The empirical formula is suggested by TGA and VTXRPD (see Fig. 8). X-Ray diffraction at variable temperature shows that [CuI(PN)$_3$] starts to transform into CuI(PN)$_2$ at 180°C and the complete transformation accompanied by amorphization is observed at 250 °C. In the TGA curve the first step which corresponds to a weight loss of 0.81% is probably due to some solvent trapped in the crystals, the second step due to the release of one ligand (calculated 26.84% weight loss) which is suddenly followed by decomposition and the release of the second and third ligand.

Photophysical properties

All complexes are luminescent in their solid state at room temperature with emissions spanning from green to orange. The tetrahedral coordination around the copper(I)ion and the stiff molecular structure assured by rigid ligands hamper the Jahn–Teller distortion of the excited state and allow high emission quantum yields.[39,40] Examination of the relevant bond angles reveals only a slightly distorted tetrahedral geometry around the Cu ions, demonstrating the fitting bite angle of the bidentate P^N ligand in the polynuclear complexes.[13] The lack of concentration quenching makes these complexes attractive for applications in solid state devices as OLEDs or LECs. Moreover their emissions stem from excited states populated by fast intersystem crossing, which allow the so-called "triplet harvesting" or "singlet harvesting" that leads to high electro- luminescence efficiencies.[13,16,41–43] The emission lifetimes are relatively short, in the order of microseconds, thus preventing excited state quenching due to triplet–triplet and triplet–charge interaction processes originating from the typical roll-off in the electroluminescence efficiency decay at high currents.[44] The frontier orbitals involved in electronic transitions have a (X+M)LCT character, only slightly affected by the halogen/metal orbital ratio contributing to the HOMO, and dependent on the CuxIx nuclearity, and by the number of bridging ligands that contribute to the LUMO. The emission spectra of the complexes that could be obtained as sufficiently pure powders are represented in Fig. 9. The dimeric $[Cu_2I_2(PN)_3]$ complex shows an emission band with maximum at 525 nm which has been assigned to a temperature assisted delayed fluorescence (TADF) from a (X+M)LCT singlet excited state in thermal equilibrium with the triplet state lying at a very close energy level.[13]

The monomer $[CuI(PN)_3]$ has a very similar emission band, most probably ascribable to a transition akin to the $[Cu_2I_2(PN)_3]$ one. None of the two compounds show radiative decay from excited states generated by cuprophilic interactions. Instead, the red-shifted and broader emission band of the $[Cu_4I_4(PN)_2{\cdot}(CH_2Cl_2)_{0.5}]$ octahedral complex is indicative of a cluster centred (CC) transition at lower energy contributing to the emission.[4]

Conclusions

Copper iodide complexes are known for their large variety of coordination geometries which allows a great deal of different stoichiometries to be attained with compounds based on the same ligand. One of the targets of the research described in this paper was that of exploring as thoroughly as possible the chemistry of CuI and the ligand diphenyl-2-pyridyl phosphine PN. Five new different compounds have been discussed: $[Cu_4I_4(PN)_2]$, $[Cu_4I_4(PN)_2{\cdot}(CH_2Cl_2)_{0.5}]$, $[CuI(PN)_{0.5}]_\infty$, $[CuI(PN)_3]$ whose structure has been determined during this study, and $CuI(PN)_2$ (see Scheme 1). Two main synthetic parameters were changed, the stoichiometry and the media in which reactions were carried out, whether in solution or the solid state. Regarding the stoichiometry, I have discovered that only by using a great excess of one of the reagents was it possible to move from the dimeric structure $[Cu_2I_2(PN)_3]$ and to obtain new compounds with higher ligand/ CuI ratios. In terms of synthetic routes I have shown that solution synthesis yielded $[Cu_4I_4(PN)_2{\cdot}(CH_2Cl_2)_{0.5}]$ and $[CuI(PN)_3]$ while $[CuI\ (PN)_{0.5}]_\infty$ and $CuI(PN)_2$ were obtained only via solid state reactions, which posed the additional problem of structure determination when only polycrystalline samples were available. One way to circumvent this problem is that of finding an alternative way to grow single crystals of the desired species. Therefore, in my study I have explored in parallel the solvothermal synthesis with CuI and PN to obtain the same species as produced by solid state reactions. In such a way I have obtained single crystals of $[Cu_4I_4(PN)_2]$ and $[CuI(PN)_{0.5}]_\infty$ which allowed full identification of this latter mechanochemical products by comparison of observed and simulated patterns. The observation that $[CuI\ (PN)_{0.5}]_\infty$ could be obtained by solid state reaction and by solvothermal methods suggests that the two processes can reach similar conditions which are not allowed in the traditional synthesis in solution. $[Cu_4I_4(PN)_2]$ and $[Cu_4I_4(PN)_2{\cdot}(CH_2Cl_2)_{0.5}]$ present very similar powder patterns which suggests that the solvated compound should maintain the same geometry, and upon thermal treatment $[Cu_4I_4(PN)_2{\cdot}(CH_2Cl_2)_{0.5}]$ converts into $[Cu_4I_4(PN)_2]$. The crystal structure of $[CuI(PN)_3]$ was solved from powder pattern X-ray diffraction data. Only the empirical formula of $CuI(PN)_2$ was postulated. This compound was obtained by ball milling or upon heating of $[CuI(PN)_3]$ at 180 °C,

which corresponds to the TGA curve at the release of one ligand. All the compounds obtained are luminescent and the photophysical properties of the complexes that could be obtained as sufficiently pure powders have been reported.

References

1. L. Bergmann, J. Friedrichs, M. Mydlak, T. Baumann, M. Nieger and S. Brase, Chem. Commun., 2013, 49, 6501–6503.
2. D. M. Zink, T. Baumann, J. Friedrichs, M. Nieger and S. Br¨ase, Inorg. Chem., 2013.
3. D.M. Zink, D. Volz, T. Baumann, M. Mydlak, H. Fl¨ugge, J. Friedrichs, M. Nieger and S. Br¨ase, Chem. Mater., 2013.
4. Z. Liu, P. I. Djurovich, M. T. Whited and M. E. Thompson, Inorg. Chem., 2012, 51, 230–236.
5. Z. Liu, M. F. Qayyum, C. Wu, M. T. Whited, P. I. Djurovich, K. O. Hodgson, B. Hedman, E. I. Solomon and M. E. Thompson, J. Am. Chem. Soc., 2011, 133, 3700–3703.
6. V. A. Krylova, P. I. Djurovich, J. W. Aronson, R. Haiges, M. T. Whited and M. E. Thompson, Organometallics, 2012, 31, 7983–7993.
7. I. Roppolo, E. Celasco, A. Fargues, A. Garcia, A. Revaux, G. Dantelle, F. Maroun, T. Gacoin, J.-P. Boilot, M. Sangermano and S. Perruchas, J. Mater. Chem., 2011, 21, 19106–19113.
8. P. P. Mazzeo, L. Maini, D. Braga, G. Valenti, F. Paolucci, M. Marcaccio, A. Barbieri and B. Ventura, Eur. J. Inorg. Chem., 2013, 4459–4465.
9. A. Barbieri, G. Accorsi and N. Armaroli, Chem. Commun., 2008, 2185–2193.
10. R. Peng, M. Li and D. Li, Coord. Chem. Rev., 2010, 254,1–18.
11. M. Vitale and P. C. Ford, Coord. Chem. Rev., 2001, 219–221,3–16.
12. P. C. Ford, E. Cariati and J. Bourassa, Chem. Rev., 1999, 99, 3625–3648.
13. D. M. Zink, M. B¨achle, T. Baumann, M. Nieger, M. K¨uhn, C. Wang, W. Klopper,U. Monkowius, T. Ho?eck, H. Yersin and S. Br¨ase, Inorg. Chem., 2013, 52, 2292–2305.
14. R. Czerwieniec, J. Yu and H. Yersin, Inorg. Chem., 2011, 50, 8293–8301.
15. D. Volz, D. M. Zink, T. Bocksrocker, J. Friedrichs, M. Nieger, T. Baumann, U. Lemmer and S. Br¨ase, Chem. Mater., 2013, 25, 3414–3426.
16. M. J. Leitl, F.-R. K¨uchle, H. A. Mayer, L. Wesemann and H. Yersin, J. Phys. Chem. A, 2013.
17. D. Volz, M. Nieger, J. Friedrichs, T. Baumann and S. Br¨ ase, Langmuir, 2013.
18. C. H. Arnby, S. Jagner and I. Dance, CrystEngComm, 2004, 6, 257–275.
19. D. J. Fife, W. M. Moore and K. W. Morse, Inorg. Chem., 1984, 23, 1684–1691.
20. CSD, 2013, Cambridge Crystallographic Data Centre, UK.
21. L. Maini, D. Braga, P. P. Mazzeo and B. Ventura, Dalton Trans., 2012, 41, 531– 539.
22. S. L. James, C. J. Adams, C. Bolm, D. Braga, P. Collier, T. Friscic, F. Grepioni, K. D. M. Harris, G. Hyett, W. Jones, A. Krebs, J. Mack, L. Maini, A. G. Orpen, I. P. Parkin, W. C. Shearouse, J. W. Steed and D. C. Waddell, Chem. Soc. Rev., 2012, 41, 413–447.
23. D. Braga, L. Maini, P. P. Mazzeo and B. Ventura, Chem.–Eur. J., 2010, 16, 1553– 1559.
24. D. Braga, F. Grepioni, L. Maini, P. P. Mazzeo and B. Ventura, New J. Chem.,

2011, 35, 339–344.
25. G. A. Bowmaker, Chem. Commun., 2013, 49, 334–348.
26. G. A. Bowmaker, J. V. Hanna, R. D. Hart, P. C. Healy, S. P. King, F. Marchetti, C. Pettinari, B. W. Skelton, A. Tabacaru and A. H. White, Dalton Trans., 2012, 41, 7513–7525.
27. G. A. Bowmaker, J. V. Hanna, B. W. Skelton and A. H. White, Chem. Commun., 2009, 2168–2170.
28. W. I. F. David, K. Shankland, L. M. McCusker and C. Baerlocher, Structure Determination from Powder Diffraction Data, Oxford University Press, New York, 2002.
29. G. A. Bowmaker and J. V. Hanna, Z. Naturforsch., Teil B, 2009, 64, 1478–1486.
30. P. J. Beldon, L. F´abi´ an, R. S. Stein, A. Thirumurugan, A. K. Cheetham and T. Fri˘sci&cacute, Angew. Chem., Int. Ed., 2010, 49, 9640–9643.
31. R. E. Morris and S. L. James, Angew. Chem., Int. Ed., 2013, 52, 2163–2165.
32. Y. Jin, Q. Sun, G. Qi, C. Yang, J. Xu, F. Chen, X. Meng, F. Deng and F.-S. Xiao, Angew. Chem., 2013, 125, 9342–9345.
33. J. F. Fernandez-Bertr´an, M. P. Hernandez, E. Reguera, H. Yee-Madeira, J. Rodriguez, A. Paneque and J. C. Llopiz, J. Phys. Chem. Solids, 2006, 67, 1612-1617.
34. C. F. Macrae, I. J. Bruno, J. A. Chisholm, P. R. Edgington, P. McCabe, E. Pidcock, L. Rodriguez-Monge, R. Taylor, J. van de Streek and P. A. Wood, J. Appl. Crystallogr., 2008, 41, 466–470.
35. G. M. Sheldrick, SHELX97, 1997, University of G¨ ottingen, Germany.
36. S. L. Childs, N. Rodriguez-Hornedo, L. S. Reddy, A. Jayasankar, C. Maheshwari, L. McCausland, R. Shipplett and B. C. Stahly, CrystEngComm, 2008, 10, 856– 864.
37. D. Volz, M. Nieger, J. Friedrichs, T. Baumann and S. Br¨ase, Inorg. Chem. Commun., 2013, 37, 106–109.
38. A. J. Blake, N. R. Brooks, N. R. Champness, P. A. Cooke, M. Crew, A. M. Deveson, L. R. Hanton, P. Hubberstey, D. Fenske and M. Schr¨oder, Cryst. Eng., 1999, 2, 181–195.
39. M. Hashimoto, S. Igawa, M. Yashima, I. Kawata, M. Hoshino and M. Osawa, J. Am. Chem. Soc., 2011, 133, 10348–10351.
40. N. Armaroli, G. Accorsi, F. Cardinali and A. Listorti, Top. Curr. Chem., 2007, 280,69–115.
41. M. A. Baldo, S. Lamansky, P. E. Burrows, M. E. Thompson and S. R. Forrest, Appl. Phys. Lett., 1999, 75,4–6.
42. M. A. Baldo, D. F. O'Brien, Y. You, A. Shoustikov, S. Sibley, M. E. Thompson and S. R. Forrest, Nature, 1998, 395, 151–154.
43. C.-W. Hsu, C.-C. Lin, M.-W. Chung, Y. Chi, G.-H. Lee, P.-T. Chou, C.-H. Chang and P.-Y. Chen, J. Am. Chem. Soc., 2011, 133, 12085–12099.
44. Highly Efficient OLEDs with Phosphorescent Materials, ed. H. Yersin, Wiley-VCH, Weinheim, 2008

Chapter 2

White luminescence achieved by a multiple thermochromic emission in a hybrid organic–inorganic compound based on 3-picolylamine and copper(I) iodide

Abstract: Three copper(I) complexes have been obtained by the reaction of CuI with 3-picolylamine in acetonitrile solution and characterized by X-ray powder diffraction, both from synchrotron and laboratory radiation. Photophysical investigations in the solid state revealed highly efficient thermally-activated delayed fluorescence (TADF) with photoluminescence quantum yields (PLQYs) up to 18%. Notably, the complex $[Cu_2I_2(3pica)]_\infty$ displays a strong luminescence thermochromism due to the presence of both ^{1,3}(X + M) LCT excited states and a lower-lying cluster-centered (^{3}CC) one, leading to multiple emission at room temperature; as a result, a white luminescence is achieved with a PLQY of 4.5%.

Introduction

Metals with d^{10} configuration are receiving increasing attention due to their potential as alternatives to Pt and Ir in OLED devices.[1,2] Among them, copper(I) halide complexes constitute a large family of compounds studied for decades for their unique photophysical and photochemical properties,[1,3–7] which are currently at the forefront of coordination chemistry and crystal engineering research.[4,7–9] The luminescent properties of copper(I) halides have captured the attention of researchers because of their varied emissive nature. Already in 1977 Hardt et al. observed a dramatic change in the emission color of these complexes with temperature (i.e., thermochromism).[10] Later, in the 90s, Ford et al. discovered that the change in color was due to two distinct emission bands, one at high-energy attributed to halide-to-ligand charge transfer (^{3}XLCT), and the other at low-energy attributed to a triplet Cu–X Cluster-Centered (^{3}CC) excited state with the excitation localized in the copper-halogen core. This behavior is only possible in the presence of interactions between the metal centers.[11] In 2011, Yersin et al. found that copper complexes are prone to present thermal activated delayed fluorescence (TADF).[12,13]

Recently, I have observed that the coordination polymer $[CuI(piperazine)_{0.5}]_\infty$ is characterized by a dual luminescence: the short copper–copper distances in the framework allow the existence of both cluster-centered and 1-D delocalized electronic transitions.[14] In addition to the richness of the emissive state nature, CuX complexes usually present high quantum yields in the solid state and do not suffer from self-quenching; in addition to that, they can be processed by solution tech- niques.[15] For all these reasons CuX complexes are promising candidates for the production of OLEDs.[16–18] Moreover, coordination systems based on copper halides show a remarkable structural diversity,[7,19] which arises from the many possible combinations of coordination numbers (two, three and four) available for copper(I) and the geometries that can be adopted by the halide ions (from terminal to μ_2- and up to μ_8-bridging).[20] This variability, while, on the one hand, gives access to different stoichiometry combinations of CuX and the ligands, hence to different compounds and different optoelectronic properties, on the other hand, makes the purposeful crystal engineering of copper halides particularly challenging.[21,22] As a matter of fact, structural characterization is

the key point to understand the properties as well as to guide the design of new compounds. A significant step ahead is represented by the growing capacity to overcome the lack of single crystals for single crystal X-ray diffraction with structure determination from powder data (XRPD), thanks to the development of "direct space" methods.[23] This approach is particularly suited for materials constructed from well-defined modular building units, while the application is more challenging for copper iodide complexes whose coordination is difficult to predict. Herein I report the synthesis of three new luminescent compounds based on copper iodide and 3-picolylamine (3pica): $[Cu_2I_2(3pica)]_\infty$, [CuI(3pica)] and $[CuI(3Pica)](CH_3CN)$. In all three cases, the compounds failed to give single crystals and the structures were determined from the synchrotron and laboratory XRPD data using the software EXPO 2014,[24] while for the refinement the software TOPAS 5[25] was used. The hybrid organic–inorganic compound[26,27] $Cu_2I_2(3Pica)_\infty$ is characterized by the presence of infinite double chains of CuI. Metal-containing chains of this type are of interest as a potential source of novel molecular wires.[28,29] [CuI(3Pica)] and [CuI (3Pica)](CH_3CN) are based on the Cu_2I_2 dimer bound by bridging ligands. These coordination polymers are molecular isomers since they differ on the spatial disposition of the ligands. The photophysical properties of these compounds have been studied in the solid state at different temperatures and do present some peculiarities. In fact, $[Cu_2I_2(3Pica)]_\infty$ is characterized by a multiple emission: the ^{1,3}(X + M)LCT states are responsible for the high-energy band (with emission maximum at 476 nm) and the lower one is attributed to the presence of a ^{3}CC state (with an emission centered around 630 nm). At room temperature, the concomitant presence of both bands leads to a white emission, which makes this com- pound interesting for potential application in lighting technology.[30] I attributed the origin of this multiple emission to the thermal interplay of three different emitting states (i.e., ^{1}(X + M)LCT, ^{3}(X + M)LCT and ^{3}CC). Due to the presence of such complex thermal equilibria, a mathematical evaluation of an excited-state energy diagram for $Cu_2I_2(3Pica)_\infty$ was not practically feasible; while, this was possible for the [CuI(3Pica)] analogue. In fact, the latter presents a typical TADF scenario with only one emission band at any temperature (in the range between 77 and 340 K), which slightly shifts to higher energy when the

temperature increases due to thermal equilibration between the singlet and triplet (X + M)LCT states. A similar, but less pronounced, behavior was also observed for [CuI(3Pica)](CH_3CN). Notably, in the case of this last com- pound, the presence of solvent molecules in the crystal lattice stiffens the complex structure leading to an increase of the emission quantum yield, which reaches 18% at 298 K.

Results and discussion

Determining the crystalline structure from powder diffraction data gives the possibility to overcome the lack of suitable single crystals for SCXRD. The key points for the structure solution from powder diffraction data are mainly the following: (i) determination of the unit cell and space group and (ii) structure solution via the simulated annealing method starting from the molecular building units. The goodness of the unit cell found can be verified by the figure of merit (FOM) and the comparison of the cell volume with the molecular volume.31 In our case I did not know the molecular volume, since the CuI : ligand stoichiometry ratio in the structure cannot be assumed from the synthesis. The cells with the best FOM were used to guess the stoichiometry ratio and the result was com- pared with the TGA curves. The weight losses before 300 °C are usually assigned to the release of the ligand and the release of solvent molecules. The simulated annealing was performed with the copper and the iodide atoms unbound and the ligand described with a rigid body. In the case of [CuI(3pica)](CH_3CN), the first solution was performed without the solvent molecule. The structure presented voids with a volume com- parable with an acetonitrile molecule, which was added during a second solution and refined with the Rietveld method. Crystallographic data for all the three compounds are summarized in Table 1.

Crystal structure of $[Cu_2I_2(3pica)]_\infty$

The crystalline structure of $[Cu_2I_2(3Pica)]_\infty$ is characterized by an infinite double chain of CuI (Fig. 1a), where the tetrahedral coordination of the copper(I) ions is fulfilled by three adjacent iodide ions and the ligand. Two copper atoms are present in the asymmetric unit: Cu1 coordinated by the aromatic N and Cu2 coordinated by the amino group. The inversion centers correlate the copper atoms within the pairs Cu1–Cu1, with a distance of 2.754(3) Å, and Cu2–Cu2, with a distance of 2.867(3) Å (Fig. 1b). The distance between Cu1 and Cu2 is 3.124(3) Å. Along the same chain the ligands are organized in an anti- parallel manner and two neighboring copper ions bind the ligand moieties alternatively by the pyridine ring and the amino group to form a bi-dimensional sheet network (Fig. 1b). These layers run parallel to the [001] direction, which allows inter-layer π–π interactions among the ligand aromatic rings as shown in Fig. 1c.

Crystal structure of [CuI(3pica)]

The crystalline structure of the compound [CuI(3pica)] reveals a 1D-cordination polymer based on a discrete flat Cu_2I_2 dimeric unit with the ligand acting as a bridge between the dimers (Fig. 2a). The copper–copper distance is 3.086(3) Å, quite long for metallophilic interactions. In fact, cuprophilicity has been investigated by different computational methods; compounds with Cu···Cu distance slightly longer than 3 Å may present bonding interactions but it is not systematically observed.

	$[Cu_2I_2(3Pica)]_\infty$	[CuI(3Pica)]	[CuI(3Pica)](CH$_3$CN)
Chemical formula	$Cu_2I_2C_6H_8N_2$	$CuIC_6H_8N_2$	$CuIC_8H_{11}N_3$
Formula Mass	489.04	298.59	339.64
Crystal System	Triclinic	Monoclinic	Monoclinic
a/Å	9.942(3)	8.343(1)	9.3432(2)
b/Å	7.608(2)	13.829(3)	14.4585(3)
c/Å	7.637(4)	7.26(1)	8.0178(2)
α/°	99.0(1)	90	90
β/°	96.25(4)	98.42°(1)	90.463(2)
γ/°	108.86(2)	90	90
Volume/ Å^3	532.08(2)	829.3(2)	1083.13(2)
Temperature	RT	RT	RT
Space group	P-1	P2$_1$/c	P2$_1$/n
R_p	0.041	0.054	0.037
R_{wp}	0.057	0.067	0.047

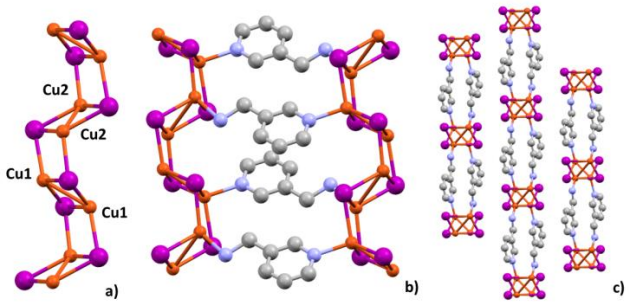

Fig. 1: a) the Cu-I chain in $[Cu_2I_2(3pica)]_\infty$, b) bi-dimensional sheet network in $[Cu_2I_2(3pica)]_\infty$, c) inter-layers π-π interactions among ligand aromatic rings add plane distances and center shift by 3.876(3) Å .

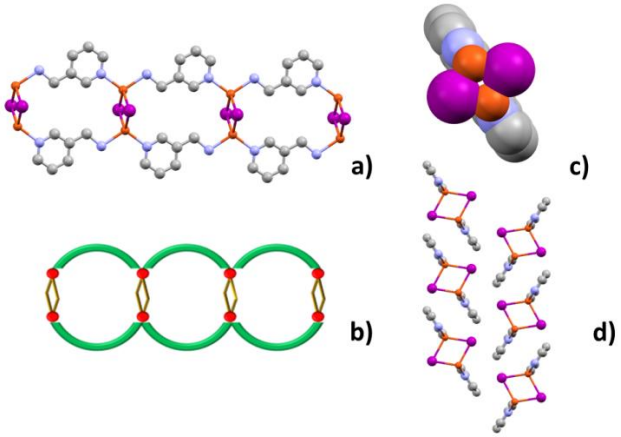

Fig. 2: a) shematic representation of the 1D-cordination polymer b) Cu_2I_2 cores wich run parallel to each other face-to-face in crystalline [CuI(3pica)]; c) cross-shape geometry; d) herring bone – type packing.

The topological features, in this context, are not enough to confirm the presence of a metallophilic interaction.[32–34] [CuI(3pica)] is characterized by only one emission band assignable to (metal + halide)-to-ligand charge transfer (see later), which is consistent with the absence of metallophilic interactions. In Fig. 2b, the bridging role of the ligand is schematized. Each copper is linked by picolylamine molecules to two different copper atoms (Fig. 2b). The Cu_2I_2 cores are perpendicular with respect to the planar bridging ligands, which give to the section of the chain a cross shaped geometry (Fig. 2c). The chains develop along the a-axes and pack themselves in a herringbone manner (Fig. 2d); this type of spatial distribution leads to the formation of several CH–π, CH–I and NH_2–I interactions.

Crystal structure of [CuI(3pica)] (CH_3CN)

The crystalline structure of [CuI(3pica)](CH_3CN) reveals a 1D- cordination polymer made by Cu_2I_2 dimeric units with the ligand acting as a bridge between the dimers (Fig. 3a). Unlike [CuI(3pica)], two picolylamine molecules share the same adjacent copper atoms as clearly schematized in Fig. 3b

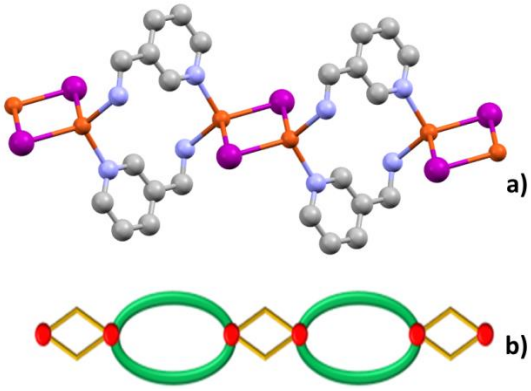

Fig. 3: a) dimeric cores bridged alternately by the amino and the pyridine group of the ligand in crystalline [CuI(3pica)](CH_3CN); b) schematic representation of the chain.

It is worth noting that [CuI(3pica)](CH_3CN) and [CuI(3pica)] present the same coordination disposition around the copper atom but the overall packing make them structural isomers. As in [CuI(3pica)], metallophilic interactions are probably absent in [CuI(3pica)](CH_3CN) since the copper–copper distance is

3.090(4) Å and the photophysical analysis which reveals the presence of only the ^{1,3}(X + MLCT) emission band. The molecules of the solvent are displaced in a herringbone manner and form interactions with the amino group of the ligand ensuring stability to the complex (Fig. 4). The variable temperature X-ray diffraction analysis evidences the stability given by the interactions with the solvent molecules. The amorphization of the complex, due to the loss of solvent is observed at 170 °C (Fig. 3b ESI†).

Photophysical properties

The photophysical properties of $[Cu_2I_2(3pica)]_\infty$, [CuI(3pica)] and $[CuI(3pica)](CH_3CN)$ were investigated in the solid state as neat powders on quartz slides, both at 298 and 77 K. All compounds are highly stable over months and do not require to be stored under oxygen-free environment. No degradation is observed under standard experimental conditions, including

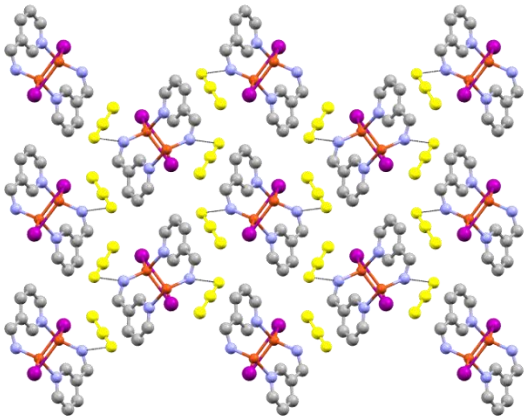

Fig. 4: solvent molecules (yellow) and amino group interactions (black lines).

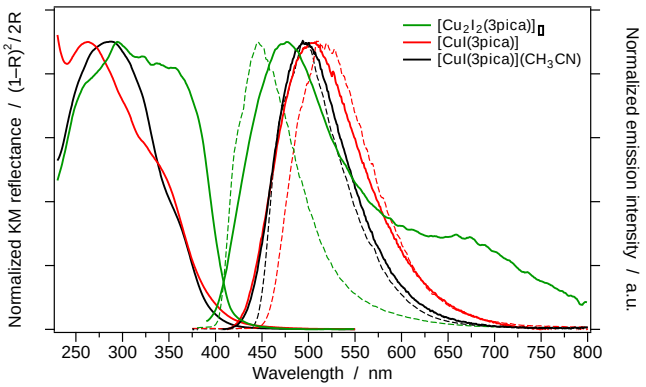

Fig. 5: Left axis: Room-temperature normalized diffuse reflectance (R) spectra of all the investigated Cu(I) complexes, elaborated using the Kubelka–Munk (KM) function. Right axis: Normalized emission spectra at 298 K (full) and at 77 K (dashed lines). All samples are in solid state (neat powder on quartz slides).

irradiation. All the related photophysical data are reported in Fig. 5 and summarized in Table 2. All compounds are luminescent at room temperature and display an unstructured greenish emission (see Fig. 5 and Table 2) assignable to the radiative deactivation of the lowest (metal + halide)-to-ligand charge transfer excited state of singlet spin multiplicity (i.e., ^{1}(X + M)LCT) in thermal equilibrium with the corresponding triplet state.[3] This type of emission is also commonly observed in other similar copper(I) iodide complexes with aromatic ligands.16 Actually, in the case of $[Cu_2I_2(3pica)]_\infty$, a second emission band is also observed at a longer wavelength (>600 nm) due to the presence of a lower- lying cluster-centred (^{3}CC) state, having a lifetime of 3.2 μs (Table 2).[35,36] The excitation spectra recorded at both the ^{1,3}(X + M)LCT and 3CC emission maxima are superimposable with the diffuse reflectance spectrum of $[Cu_2I_2(3pica)]_\infty$ (see Fig. 4 ESI†), ruling out the presence of impurities or spurious emissions. The ^{3}CC state only exists in $[Cu_2I_2(3pica)]_\infty$ because of the presence of the infinite double chain of CuI with a Cu–Cu distance of approx. 2.78 Å (see above); in fact, at this distance, copper–copper interactions can easily take place, possibly originating CC states.[37] On the contrary, the Cu–Cu distance in [CuI(3pica)] and [CuI(3pica)] (CH_3CN) is much longer (i.e., 3.086 and 3.090 Å, respectively), so that a cuprophilic interaction can be ruled out, as well as the presence of lower-lying CC states.

As far as photoluminescence quantum yields (PLQYs) are concerned, it should be underlined that [CuI(3pica)](CH_3CN) displays a 7-fold increase in the PLQY

when compared to its structural isomer [CuI(3pica)] (i.e., 18.4% vs. 2.8%, see Table 2). This could be rationalized since the crystal structure of these two isomers (see above). In fact, the presence of the interaction between the amine substituent of the 3-picolyl- amine ligands and the acetonitrile molecules in [CuI(3pica)] (CH_3CN) results in an increased stability and a more rigid structure of the crystal, leading to less geometrical distortions in the excited state. The absence of any spectral shift upon lowering the temperature to 77 K further supports this hypothesis (see Table 2). As a consequence, a negligible energy difference between the lowest singlet state (S1 or ^{1}(X + M)LCT, in this case) and the lowest triplet state (T1 or ^{3}(X + M)LCT) is expected; in fact, while the former is mainly responsible for the emission at room temperature, the latter is assumed to be predominant at 77 K.[16] Anyway, due to the virtually non-existent energy difference between S1 and T1, singlet harvesting is thermally feasible in [CuI (3pica)](CH_3CN) even at low temperatures, which leads to very fast radiative deactivations, as demonstrated by the radiative constant (kr) that is one order of magnitude greater than in [CuI (3pica)]. As a consequence, since the non-radiative constants (knr) are comparable between the two compounds, PLQYs are 7times higher in the case of [CuI(3pica)](CH_3CN), when compared to its solvent-free analogue. In the case of [CuI(3pica)], the energy difference between S1 and T1 is expected to be much greater, as one would estimate comparing the emission maxima at low and room temperature (see Fig. 5 and Table 2). In fact, at 77 K, the excited-state life- time of [CuI(3pica)] is 62 μs (to be compared with 12 μs for [CuI(3pica)](CH_3CN), see Table 2) and therefore the emission can be attributed, almost exclusively, to the lowest triplet state (T1) with no contribution from singlet harvesting. On the other hand, at 298 K, the same compound shows a lifetime of 7.9 μs and a blue shift of the emission, when compared to 77 K data (see Table 2). These experimental findings suggest the presence of a thermally-activated delayed fluorescence (TADF) at room temperature, allowing radiative deactivations also from the lowest singlet excited state (S1) of [CuI(3pica)] (see below).

Thermally-activated delayed fluorescence (TADF)

To get a deeper insight into the photophysical properties of [CuI(3pica)] and of a possible TADF mechanism, the emission spectra and lifetimes of [CuI(3pica)] (as neat powder) have been investigated at different temperatures (from 78 to 338 K, see Fig. 6).

Table 2: Photophysical parameters for $[Cu_2I_2(3pica)]_\infty$, [CuI(3pica)] and $[CuI(3pica)](CH_3CN)$, as neat powder at 298 K and at 77 K (values in bracket).

	λ_{em} [a] [nm]	PLQY [%]	τ [b] [μs]	k_r [c] [10^4 s^{-1}]	k_{nr} [d] [10^4 s^{-1}]
$[Cu_2I_2(3pica)]_\infty$	476, 630[sh] (446)	4.5 [e]	0.9, 3.2 [f] (3.4)	--- [g]	--- [g]
[CuI(3pica)]	500 (514)	2.8 [e]	7.9 (62)	0.35	12
[CuI(3pica)] (CH_3CN)	495 (497)	18.4 [e]	5.0 (12)	3.7	16

[a] Emission maximum from corrected spectra. [b] Emission lifetime measured at emission maximum. [c] k_r = PLQY/τ . [d] $k_{nr} = 1/\tau - k_r$. [e] Absolute PLQY determined using an integrating sphere in air-equilibrated environment. [f] Emission lifetime at 650 nm (*i.e.*, on the cluster-centred band). [g] Kinetic constant not evaluable due to the presence of multiple emitting states with different lifetimes.

Following eqn (1), it is possible to experimentally determine the energy separation (actually the activation energy) between S1 and T1 (i.e., ΔE(S1 – T1)) and their emission lifetimes in the absence of thermal equilibrium (i.e., τ(S1) and τ(T1)).[38]

$$\tau(T) = \frac{3+\exp\left[{}^{-\Delta E(S_1-T_1)}/_{k_B T}\right]}{\frac{3}{\tau(T_1)}+\frac{1}{\tau(S_1)}\exp\left[{}^{-\Delta E(S_1-T_1)}/_{k_B T}\right]} \qquad (1)$$

Because in the investigated temperature range only single-exponential decays were observed, a fast equilibration takes place between T1 and S1 and eqn (1) can be used without further modifications.16 By fitting this equation to the experimental data reported in Fig. 6(inset), I determined the lifetime of the prompt fluorescence τ(S1) ≈ 300 ns and the decay time of the phosphorescence τ(T1)= 62 μs. It should be emphasized that the measured lifetime at 298 K, despite arising from a S1 → S0 transition, displays a lifetime that is 23 times longer than the one calculated in the absence of thermal equilibrium (e.g., 7.9 μs

vs. 340 ns, see Table 2 and Fig. 6); this is because, at room temperature, S1 is fed by the long-lived T1 reservoir, leading to the so-called delayed fluorescence. The fitting procedure also allows the evaluation of the energy separation between the two emitting states (i.e., ΔE (S1 – T1) = 0.061 eV). This value is comparable to similar copper(I) iodide bridged coordination compounds16 or other heteroleptic Cu(I) complexes with one chelating diimine and one bis-phosphine ligand.39 Notably the above-mentioned ΔE (S1 – T1)is in accordance with the energy separation between the emission maxima recorded at 77 and 298 K (i.e., 0.068 eV, derived from data in Table 2).

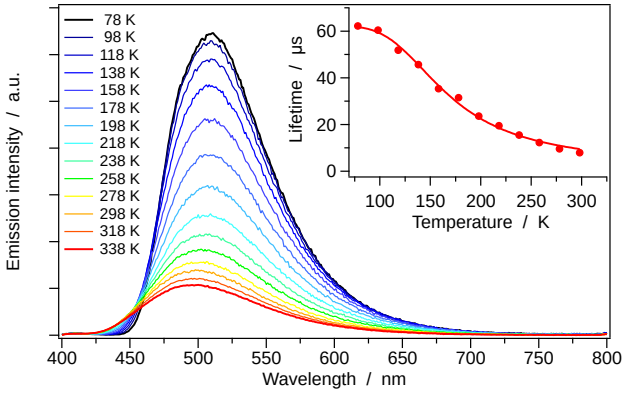

Fig. 6: Emission spectra of [CuI(3pica)] (neat powder) recorded between 78 and 338 K; the emission maximum at 338 K is 0.068 eV blue-shifted if compared to the one recorded at 78 K. Inset: temperature-dependent emission lifetimes of [CuI(3pica)] (powder); the corresponding decays are strictly monoexponential in the whole temperature range. The red curve represents a fit according to eq. 1; the parameters obtained from the fitting procedure are ΔE (T_1– S_1) = (0.061 ± 0.007) eV, $\tau(T_1)$ = (62 ± 3) µs, and $\tau(S_1)$ = (0.3 ± 0.1) µs.

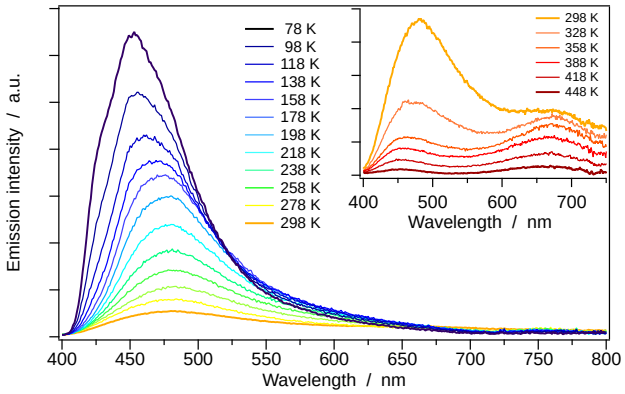

Fig. 7: Temperature-dependent emission spectra of $[Cu_2I_2(3pica)]_\infty$ (neat powder) recorded between 78 and 298 K (main graph) and between 298 and 448 K (inset).

Thermochromic luminescence of $[Cu_2I_2(3pica)]_\infty$

The $[Cu_2I_2(3pica)]_\infty$ complex, showing multiple emission bands at room temperature (Fig. 5), also deserves a more detailed photophysical investigation. As in the case of [CuI (3pica)], the emission spectra of $[Cu_2I_2(3pica)]_\infty$ (as neat powder) were investigated at different temperatures, from 78 to 448 K (see Fig. 7). At 77 K, the complex shows a blue emission originating from a single band centered at 446 nm (CIE coordinates: x = 0.172, y = 0.157; see Fig. 7). This band is attributed to the lowest ^{3}(X + M)LCT state, as indicated by the long emission lifetime (i.e., 3.4 μs, Table 2) and suggested by the temperature-dependent study I performed for the [CuI(3pica)] analogue. On the other hand, when the temperature increases, this band strongly reduces its emission intensity and a new emission arises at 675 nm. In the temperature range between approx. 100 and 300 K, the latter band is only a shoulder of the ^{1,3}(X + M)LCT band but, around 328 K, the two bands display comparable intensity. Consequently, at room temperature, $[Cu_2I_2(3pica)]_\infty$ displays a cold white emission with CIE coordinates (x = 0.277, y = 0.324) at 298 K. Only at temperature above 350 K, the lower-energy band becomes predominant (Fig. 7, inset). This band can be attributed to the population of the ^{3}CC state, as already described before and reported by P. C. Ford et al. in the early 90s for copper(I) iodide pyridine complexes.11 In ESI Fig. 5,† the color changes of the $[Cu_2I_2(3pica)]_\infty$ emission with temperature are depicted in terms of CIE co- ordinates on a chromaticity diagram. A rigorous mathematical model to evaluate an energy diagram of the electronic states involved in the excited-state deactivation of $[Cu_2I_2(3pica)]_\infty$ is extremely challenging under both theoretical and experimental points of view. In fact, the polymeric nature of $[Cu_2I_2(3pica)]_\infty$ prevents the use of conventional DFT and TD-DFT methods,[3] imposing the use of very demanding density-functional calculations based on periodic boundary conditions (PBC). Moreover, also from the experimental point of view, a straight- forward two-state model (i.e., 3(X + M)LCT vs. 3CC)[40] cannot be applied because the energy of the high-energy charge-transfer band of $[Cu_2I_2(3pica)]_\infty$ is extremely temperature dependent (see Fig. 7). This complex scenario is not at all common in thermochromic copper iodide clusters; in fact, in many temperature-dependent

investigations it is commonly observed that the higher-energy band of copper(I) iodide clusters does not shift with temperature and only its emission intensity is affected by the thermally activated population of the lowest ^{3}CC state.[8,41,42] I reasonably attribute the peculiar photophysical behaviour of $[Cu_2I_2(3pica)]_\infty$ to a complex interplay between the three excited states (i.e., ^{1}(X + M)LCT, ^{3}(X + M)LCT and ^{3}CC). As for [CuI(3pica)], a fast equilibration between the singlet and triplet (X + M)LCT states occurs also in the present case; this is indicated by the remarkable reduction in the lifetime of the higher-energy band when temperature increases (i.e., 3.4 vs. 0.9 μs at 77 and 298 K, respectively; see Table 2). Anyway, the traditional blue-shift of the emission band upon temperature increase, a typical indication of TADF, is not detected (Fig. 7). In fact, a much more complicated scenario is observed: at first, the $[Cu_2I_2(3pica)]_\infty$ emission maximum displays a gradual red- shift in the range between 77 and 200 K and then, only at temperatures above 200 K, the band inverts its drift shifting to higher energy, as commonly observed in TADF (Fig. 7). Such a complex trend could be attributed to the increasing relative intensity of the emission from the 3CC state, which is thermally populated by both the ^{1,3}(X + M)LCT ones. For the sake of strictness, it must be mentioned also that the energy of the ^{3}CC state band is temperature dependent,[3,40] virtually preventing an unambiguous mathematical treatment of these complicated excited-state equilibria in $[Cu_2I_2(3pica)]_\infty$.

Experimental part

Materials and methods

General. All glassware was dried in an oven set to a temperature of 80 °C for 24 h prior to use and stripped with N2 for 15 min. All reagents were purchased from Sigma Aldrich and used without further purification.

Synthetic procedures

Synthesis of $[Cu_2I_2(3pica)]_\infty$.

CuI (3 mmol; 0.570 gr) was dissolved in 50 mL of acetonitrile at 80 °C, and when the solution turned limpid, 3-picolylamine (1 mmol; 100µL) was added with a syringe under stirring for 30 seconds. A high crystalline whitish powder precipitated at the bottom of the flask, then it was filtered on a Buckner funnel and washed with acetonitrile. Elemental analysis (%) calcd for $Cu_2I_2C_6H_8N_2$: C 14.74, H 1.65, N 5.73. Found: C 13.95, H 1.62, N 5.89.

Synthesis of [CuI(3pica)]

CuI (1 mmol; 0.190 gr) was dissolved in 15 mL of acetonitrile at 80 °C, and when the solution turned limpid, 3-picolylamine (1 mmol; 100µL) was added with a syringe under stirring for 30 seconds. A high crystalline whitish powder precipitated at the bottom of the flask, then it was filtered on a Buckner funnel and washed with acetonitrile. Elemental analysis (%) calcd for $CuIC_6H_8N_2$: C 24.13, H 2.70, N 9.38. Found: C 24.51, H 2.70, N 9.53.

Synthesis of CuI(3pica)(CH_3CN)

CuI (1 mmol) was dissolved in 20 mL of CH_3CN under stirring in a nitrogen atmosphere at room temperature. 3-Picolylamine (2 mmol; 200 µL) was diluted in 20 ml of acetone and added to the solution of CuI/ AcCN dropwise. First, a white powder, which showed a yellow/ orange luminescence, was obtained, after a few seconds the emission became pale green and it remained so until the end of the reaction. The highly crystalline whitish powder which was

precipitated at the bottom of the flask was filtered on a Buckner funnel and washed with acetonitrile. Elemental ana- lysis (%) calcd for $CuIC_8H_{11}N_3$: C 28.29, H 3.26, N 12.37. Found: C 28.76, H 3.24, N 11.56.

Synchrotron radiation X-ray powder diffraction analysis

Synchrotron radiation-XRPD measurements of $[CuI(3pica)](CH_3CN)$ and [CuI(3pica)] were performed at the Swiss Light Source (SLS) Material Science (MS) Powder Diffraction (PD) end station43 with a nominal photon energy of 16 keV. Fine Si640D NIST standard refinement returned a wavelength of 0.775375(2) Å and a residual zero error of −0.0253(4) 2θ. Data were collected with a 1D Mythen II detector[44] in the range of 2–120 2θ with an intrinsic step size of 0.0036 (2θ). Samples were loaded in 0.3mm glass capillaries and spun at 4 Hz during the measurement. Multiframing data were recorded in trans- mission with an exposure time of 5 seconds to avoid radiation damage; the raw data were then individually inspected before being merged together and flat field corrected. Expo 14[24] was used for structure determination in direct space. The best solution was chosen for a Rietveld refinement that was performed using the software TOPAS 5[25] against the original data set and gave a good final fit summarized in Table 2. A Chebyshev function and a pseudo Voigt (TCHZ type) were used to fit the back- ground and the peak shape respectively. In the refinement step, the ligand torsion angles were restrained according to CSD stat- istics and the coordination bonds were forced to be coherent to copper(I) pseudo-tetrahedral geometry. In the figures below are shown the Rietveld analysis plots for the three samples (Fig 8: $[CuI(3pica)]_2$, Fig 9: $[CuI(3pica)](CH_3CN)$, Fig 10: $[Cu_2I_2(3pica)]_\infty$). Red line is the calculated diffractogram, blue line is the observed diffractogram and grey line is the difference plot.

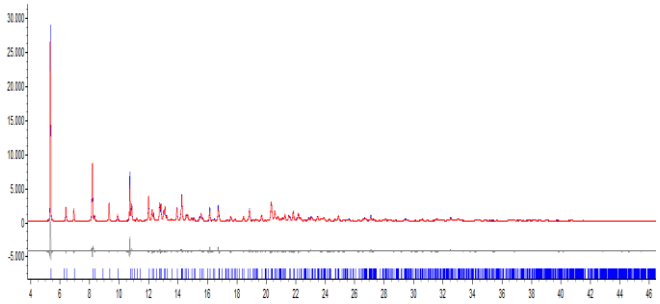

Fig. 8: Rietveld analysis plot of Cu_2I_2(3pica). Red line is the calculated diffractogram, blue line is the observed diffractogram and grey line is the difference plot

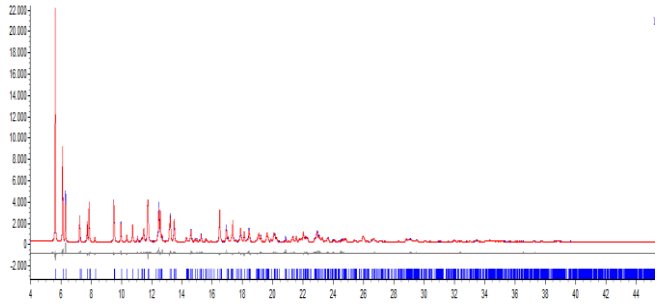

Fig. 9: Rietveld analysis plot of CuI(3pica)(CH_3CN). Red line is the calculated diffractogram, blue line is the observed diffractogram and grey line is the difference plot

X-ray powder diffraction analysis

The powder of $[Cu_2I_2(3pica)]_\infty$ is particularly sticky and it was not possible to fill up a capillary. X-Ray powder diffractograms were collected in refection geometry in a flat sample holder, over the range of 3–70° 2θ (40 mW–40 mA; Cu-Kα radiation, step size 0.00836°) on a Panalytical X'Pert PRO automated diffractometer with CuKα radiation equipped with an X'Celerator detector.

Variable temperature X-ray powder diffraction

The data were collected in open air in Bragg–Brentano geometry using Cu-Kα radiation without a monochromator. X-ray powder diffractograms were collected in the 2θ range of 5–50° using a Panalytical X'Pert PRO automated diffractometer equipped with an X'Celerator detector and an Anton Paar TTK 450 system for measurements at a controlled temperature.

Thermogravimetric analysis (TGA)

TGA measurements were performed using a Perkin Elmer TGA7 in the temperature range of 35–400 °C under a N2 gas flow and heating was carried out at 5 °C min−1.

Photophysical measurements

All the spectroscopic investigations were carried out in the solid state (powder) using quartz slides or tubes as holders. Difffuse reflectance spectra were recorded using a PerkinElmer Lambda 950 spectrophotometer equipped with a 100 mm Spectralon®-coated integrating sphere and a R928 photomultiplier tube (PMT) as a detector. The uncorrected emission spectra were obtained with an Edinburgh Instruments FLS920 spectrometer equipped with a Peltier-cooled Hamamatsu R928 PMT. An Edinburgh Xe 900 (450 W xenon arc lamp) was used as the excitation light source. The corrected spectra were obtained via a calibration curve supplied with the instrument. To record the 77 K luminescence spectra, samples were placed in quartz tubes (2 mm inner diameter) and inserted into a special quartz Dewar flask filled with liquid nitrogen. Photoluminescence quantum yields (PLQYs) were calculated by corrected emission spectra obtained from the above-mentioned Edinburgh FLS920 spectrometer equipped with a barium sulfate-coated integrating sphere (a diameter of 4 in.) following the procedure described by Würth et al.45 The emission lifetimes (τ) were measured through the time-correlated single photon counting (TCSPC) technique using an HORIBA Jobin Yvon IBH

FluoroHub controlling a spectrometer equipped with a NanoLED (λexc = 330 nm) or a laser diode (λexc = 407 nm) as pulsed excitation sources and a red-sensitive Hamamatsu R-3237-01 PMT as a detector. The analysis of the luminescence decay profiles was accomplished with DAS6 Decay Analysis Software provided by the manufacturer, and the quality of the fitting was assessed with the $\chi 2$ value close to unity and with the residuals regularly distributed along the time axis. Samples were excited at both 350 and 375 nm for the evaluation of PLQYs and at 330 and 407 nm for determinations. For temperature-dependent measurements, the sample was mechanically dispersed on a quartz slide and placed inside an Oxford Optistat DN variable-temperature liquid-nitrogen cryostat (operating range: 77–500 K) equipped with an ITC5035 temperature controller and interfaced with the afore mentioned Edinburgh FLS920 spectrometer. Experimental uncertainties are estimated to be ±10% for determinations, ±20% for PLQYs, ±2 nm and ±5 nm for absorption and emission peaks, respectively.

Conclusions

In this section of the thesis, I have reported the synthesis of three new luminescent compounds based on CuI and 3-(picolylamine) with promising photophysical properties. All the structures were solved in direct space from powder X-ray diffraction data from both synchrotron and laboratory radiation. The difficulties in controlling the coordination of the copper and iodide ions made structure determination particularly challenging. The coordination polymers [CuI(3Pica)] and [CuI(3Pica)](CH_3CN) are characterized by the presence of only ^{1,3}(X + M) LCT excited states, since no cuprophilic interactions are observed. In particular [CuI(3Pica)] presents a classical TADF scenario in which a blue shift of the emission band is observed as the temperature increases, due to thermal equili- bration between the singlet and triplet (X + M)LCT states. A similar, but less pronounced, behavior was also observed for [CuI(3Pica)](CH_3CN). Notably, in the case of this latter com- pound, the presence of solvent molecules in the crystal lattice stiffens the complex structure leading to an increase of the emission quantum yield, which reaches 18% at 298 K. The hybrid organic–inorganic $[Cu_2I_2(3pica)]_\infty$ has potential application in lighting technology since it is a white emitter due to the concomitant presence at room temperature of a high- energy and a low-energy emission band (with emission maximum at 476 and 630 nm, respectively). Since the high- energy band is attributed to two different emitting states in thermal equilibrium (i.e. ^{1}(X + M)LCT and ^{3}(X + M)LCT), $[Cu_2I_2(3pica)]_\infty$ is likely characterized by a concomitant triple emission at room temperature, which has never been described before for other copper(I) iodide compounds.

References

1. 1T. Hofbeck, U. Monkowius and H. Yersin, J. Am. Chem. Soc., 2015, 137, 399–404.
2. Z. Liu, M. Qayyum, C. Wu, M. T. Whited, P. I. Djurovich, K. O. Hodgson, B. Hedman, E. I. Solomon and M. E. Thompson, J. Am. Chem. Soc., 2011, 133, 3700–3703.
3. F. De Angelis, S. Fantacci, A. Sgamellotti, E. Cariati, R. Ugo and P. C. Ford, Inorg. Chem., 2006, 45, 10576–10584.
4. C. H. Arnby, S. Jagner and I. Dance, CrystEngComm, 2004, 6, 257–275.
5. E. Cariati, E. Lucenti, C. Botta, U. Giovanella, D. Marinotto and S. Righetto, Coord. Chem. Rev., 2015, 306, 566–614.
6. -P. C. Ford, E. Cariati and J. Bourassa, Chem. Rev., 1999, 99, 3625–3647.
7. R. Peng,M. Li and D. Li, Coord. Chem. Rev.,2010, 254,1–18.
8. Q. Benito, X. F. Le Goff, G. Nocton, A. Fargues, A. Garcia, A. Berhault, S. Kahlal, J.-Y. Saillard, C. Martineau, J. Trébosc, T. Gacoin, J.-P. Boilot and S. Perruchas, Inorg. Chem., 2015, 54, 4483–4494.
9. K. Tsuge, Y. Chishina, H. Hashiguchi, Y. Sasaki, M. Kato, S. Ishizaka and N. Kitamura, Coord. Chem. Rev., 2016, 306, 636–651.
10. H. D. Hardt and A. Pierre, Inorg. Chim. Acta, 1977, 25, L59– L60.
11. C. K. Ryu, M. Vitale and P. C. Ford, Inorg. Chem., 1993, 32, 869–874.
12. R. Czerwieniec, J. Yu and H. Yersin, Inorg. Chem., 2011, 50, 8293–8301.
13. D. M. Zink, M. Bächle, T. Baumann, M. Nieger, M. Kühn, C. Wang, W. Klopper, U. Monkowius, T. Hofbeck, H. Yersin and S. Bräse, Inorg. Chem., 2013, 52, 2292–2305.
14. L. Maini, D. Braga, P. P. Mazzeo, L. Maschio, M. Rerat, I. Manet and B. Ventura, Dalton Trans., 2015, 44, 13003– 13006.
15. D. Volz, M. Wallesch, S. L. Grage, J. Göttlicher, R. Steininger, D. Batchelor, T. Vitova, A. S. Ulrich, C. Heske, L. Weinhardt, T. Baumann and S. Bräse, Inorg. Chem., 2014, 53, 7837–7847.
16. M. J. Leitl, F. R. Küchle, H. A. Mayer, L. Wesemann and H. Yersin, J. Phys. Chem. A, 2013, 117, 11823–11836.
17. G. M. Farinola and R. Ragni, Chem. Soc. Rev., 2011, 40, 3467–3482.
18. Z. Liu, J. Qiu, F. Wei, J. Wang, X. Liu, M. G. Helander, S. Rodney, Z. Wang, Z. Bian, Z. Lu, M. E. Thompson and C. Huang, Chem. Mater., 2014, 26, 2368–2373.
19. C. Slabbert and M. Rademeyer, Coord. Chem. Rev., 2015, 288,18–49.
20. D. Braga, F. Grepioni, L. Maini, P. P. Mazzeo and B. Ventura, New J. Chem., 2011, 35, 339–344.
21. L. Maini, P. P. Mazzeo, F. Farinella, V. Fattori and D. Braga, Faraday Discuss., 2014, 170,93–107.
22. L. Maini, D. Braga, P. P. Mazzeo and B. Ventura, Dalton Trans., 2012, 41, 531–539.
23. W. I. F. David, K. Shankland, K. D. M. Harris, M. Tremayne, J. van de Streek, E. Pidcock, W. D. S. Motherwell and J. C. Cole, Acta Crystallogr., Sect. A: Fundam. Crystallogr., 2006, 39, 910–915.
24. A. Altomare, M. Camalli, C. Cuocci, C. Giacovazzo and A. G. G. Moliternia, J. Appl. Crystallogr., 2009, 42, 1197– 1202.
25. A. Coelho, Topas Academic Version 5, Computer Software, Brisbane, 2013.
26. E. Cariati, E. Lucenti, C. Botta, U. Giovanella, D. Marinotto and S. Righetto, Coord. Chem. Rev., 2016, 306, 566–614.
27. C. Janiak, Dalton Trans., 2003, 101, 2781.
28. M. Mitsumi, in Material Designs and New Physical Properties in MX- and MMX-Chain Compounds, Springer, Vienna, 2013, pp. 151–205.

29. K. Hassanein, J. Conesa-Egea, S. Delgado, O. Castillo, S. Benmansour, J. I. Martínez, G. Abellán, C. J. Gómez- García, F. Zamora and P. Amo-Ochoa, Chem. – Eur. J., 2015, 21, 17282–17292.
30. P. P. Mazzeo, L. Maini and D. Braga, RM2014A000244, 2003–2004.
31. W. I. F. David and K. Shankland, Acta Crystallogr., Sect. A: Fundam. Crystallogr., 2008, 64,52–64.
32. S. Dinda and A. G. Samuelson, Chem. – Eur. J., 2012, 18, 3032–3042.
33. M. A. Carvajal, S. Alvarez and J. J. Novoa, Chem. – Eur. J., 2004, 10, 2117–2132. 17946
34. A. C. Tsipis, Coord. Chem. Rev., 2016, DOI: 10.1016/ j.ccr.2016.08.005.
35. J. P. Safko, J. E. Kuperstock, S.M.McCullough, A. M. Noviello, X. Li,J.P.Killarney,C.Murphy, H. H. Patterson, C. A. Bayse andR.D.Pike, Dalton Trans., 2012, 41, 11663–11674.
36. P. P. Mazzeo, L. Maini, A. Petrolati, V. Fattori, K. Shankland and D. Braga, Dalton Trans., 2014, 43, 9448–9455.
37. E. Cariati, J. Bourassa and P. C. Ford, Chem. Commun., 1998, 1623–1624.
38. M. Osawa, M. Hoshino, M. Hashimoto, I. Kawata, S. Igawa and M. Yashima, Dalton Trans., 2015, 44, 8369–8378.
39. C. L. Linfoot, M. J. Leitl, P. Richardson, A. F. Rausch, O. Chepelin, F. J. White, H. Yersin and N. Robertson, Inorg. Chem., 2014, 53, 10854–10861.
40. F. Parmeggiani and A. Sacchetti, J. Chem. Educ., 2012, 89, 946–949.
41. S. Perruchas, C. Tard, X. F. Le Goff, A. Fargues, A. Garcia, S. Kahlal, J.-Y. Saillard, T. Gacoin and J.-P. Boilot, Inorg. Chem., 2011, 50, 10682–10692.
42. I. Roppolo, E. Celasco, A. Fargues, A. Garcia, A. Revaux, G. Dantelle, F. Maroun, T. Gacoin, J.-P. Boilot, M. Sangermano and S. Perruchas, J. Mater. Chem., 2011, 21, 19106–19113.
43. P. R. Willmott, D. Meister, S. J. Leake, M. Lange, A. Bergamaschi, M. Böge, M. Calvi, C. Cancellieri, N. Casati, A. Cervellino, Q. Chen, C. David, U. Flechsig, F. Gozzo, B. Henrich, S. Jäggi-Spielmann, B. Jakob, I. Kalichava, P. Karvinen, J. Krempasky, A. Lüdeke, R. Lüscher, S. Maag, C. Quitmann, M. L. Reinle-Schmitt, T. Schmidt, B. Schmitt, A. Streun, I. Vartiainen, M. Vitins, X. Wang and R. Wullschleger, J. Synchrotron Radiat., 2013, 20, 667–682.
44. A. Bergamaschi, A. Cervellino, R. Dinapoli, F. Gozzo, B. Henrich, I. Johnson, P. Kraft, A. Mozzanica, B. Schmitt and X. Shi, J. Synchrotron Radiat., 2010, 17, 653–668.
45. C. Würth, M. Grabolle, J. Pauli, M. Spieles and U. Resch- Genger, Nat. Protoc., 2013, 8, 1535–1550.

Chapter 3

Some highlights on the luminescent properties of mono and double chain structures of the Copper Iodide and pyrazine coordination polymers.

Abstract: Three copper iodide coordination polymers have been obtained from the reaction of CuI with pyrazine. Together with the already known double chain polymer $[Cu_2I_2(pyz)]_\infty$ I have prepared the new extended network $[CuI(pyz)]_\infty$ and the molecular compound [CuI(pyz)]. The three systems can be recognized on the basis of the different powder color: yellow, red and orange, respectively. The structure of the $[CuI(pyz)]_\infty$ is characterized by infinite chains of CuI bridged by the pyrazine ligands. By heating up to 110°C, $[CuI(pyz)]_\infty$ and [CuI(pyz)] convert into $[Cu_2I_2(pyz)]_\infty$, which converts back in to the starting compounds upon kneading or grinding in the presence of pyrazine. The photophysical measurements describe the particular behavior of $[Cu_2I_2(pyz)]_\infty$, the emission maximum at RT can move from 664nm in powder samples to 588nm in crystals. I hypothesized that the two emission band corresponds to two different emissive states and in presence of high crystallinity the low energy band could not be populated.

Introduction

The synthesis of coordination polymers based on the combination of metal ions and ligands (organic or inorganic) have gained a great deal of attention because of potential applications as multifunctional and dynamic materials. The final properties can be tuned by an appropriate design of ligands and of metals.[1-3] The quest for more sustainable materials has driven the studies towards the use of coinage metals, which are cheaper and more environmental friendly than Ir, Pt and rare earth metal ions.[4-6] Among them the family of copper(I) halides and pseudo-halides is particularly attractive due to its large variety of photophysical properties[7-10] associated with an extremely high structural diversity.[11] This latter feature implies, as a drawback, that the final structure of the coordination polymer based on Cu(I) is difficult to design. The organic ligand and the nature of the halide seem to have small influence of the final structure since it is possible to synthesis several different compounds with the same reagents, for instance, there are not less than 13 different structures in the CSD[12] based CuI and DABCO (diazabicyclo octane) which differ in stoichiometry, nuclearity of the CuI core and nature of solvent molecules.[13] On the other hand, the synthetic conditions are important for the final product. Reactions performed with an excess of ligand favour the formation of low nuclearity compounds such as dimers. If the ligand is bidentate, it is possible to obtain coordination polymer, while reactions performed with an excess of Cu(I)X induce to the formation infinite 1-D or 2-D inorganic polymers, which in turn can be connected via organic ligand. Moreover reactions in solution, solvothermal conditions or by mechanochemistry lead to different results.[14-15]

Recently, the presence of infinite double chain based on Copper halide or pseudo-halides have been investigated for their luminescence[16-18] and conductivity properties.[19-24] In the case of CuI with piperazine I have demonstrated that the presence of a short Copper- Copper distances within the CuI double chain allows a dual emission.[25]

In the quest of new candidate for 1-D delocalized orbital, I have focused our attention on the coordination polymer based on copper iodide and pyrazine $[Cu_2I_2(pyz)]_\infty$ whose structure present short Copper-Copper distances.[26]

Here I report the novel structure based on CuI and pyrazine $[CuI(pyz)]_\infty$ which exhibits a broad luminescence up to the Near Infrared Region. The $[CuI(pyz)]_\infty$ structure, a missing piece in a recent work published by Kharti et al.,[15] was obtained by kneading and recrystallization by solvothermal conditions. The photophysical studies on this compound as well as on the known $[Cu_2I_2(pyz)]_\infty$ [26] allowed me to highlight on an interesting behaviour in the emission properties influenced by crystallinity. I also discovered that $[CuI(pyz)]_\infty$ can transform reversibly into $[Cu_2I_2(pyz)]_\infty$ by simply increasing the temperature at 110°C and losing a pyrazine molecule. Reversibly, grinding $[Cu_2I_2(pyz)]_\infty$ with an excess of pyrazine rebalances the structural stoichiometry and induces the formation of the compound $[CuI(pyz)]_\infty$. During my investigation I was also able to obtain a new elusive phase [CuI(pyz)] which readily transforms into $[Cu_2I_2(pyz)]_\infty$.

Results and discussion

The copper iodide was reacted with pyrazine with different synthetic procedures which differ mainly for the stoichiometric ratio or for the aggregation state (solid state or solution). The reactions in solution are carried out in acetonitrile or saturated aqueous solution of KI in air, while the reactions in solid state were carried out via ball milling with few drops of acetonitrile. Three different compounds have been isolated so far, $[Cu_2I_2(pyz)]_\infty$ already described by Champness et al.,[26] $[CuI(pyz)]_\infty$ whose structure has been determined by me and [CuI(pyz)] whose structure is still under investigation. The compounds $[CuI(pyz)]_\infty$ and $[Cu_2I_2(pyz)]_\infty$ can be obtained via kneading with acetonitrile with 1:4 and 2:1 stoichiometric ratio respectively while crystals suitable for X-ray diffraction were obtained via solvothermal reaction and liquid diffusion respectively. It is worth noting that the crystals of $[CuI(pyz)]_\infty$ are only obtainable via solvothermal and every other attempts to obtain the same result via solution failed. The third compound was obtained only as microcrystalline powder; all attempts to wash or improve the crystallinity leaded to $[Cu_2I_2(pyz)]_\infty$.

Crystal structure of [CuI(pyz)]∞

The structure of [CuI(pyz)]∞ consists of "zig-zag" chains of CuI in which the copper atoms, in tetrahedral coordination, bind two iodine atoms and two pyrazine molecules. The chains are linked together by the ligand which act as a bridge between two copper atoms forming an infinite 2-D network (fig 1a). The crystal packing reveals the presence of stratified sheets along the b-axes (fig 1b). Because of the presence of only one CuI chain it is not possible to bring Cu-atom at a distance that allows the ^{3}CC emission band. This structure is isomorphous to the previous reported [CuX(pyz)]∞ with X=Cl, Br. [28-31] Main crystallographic data are reported in table 1.

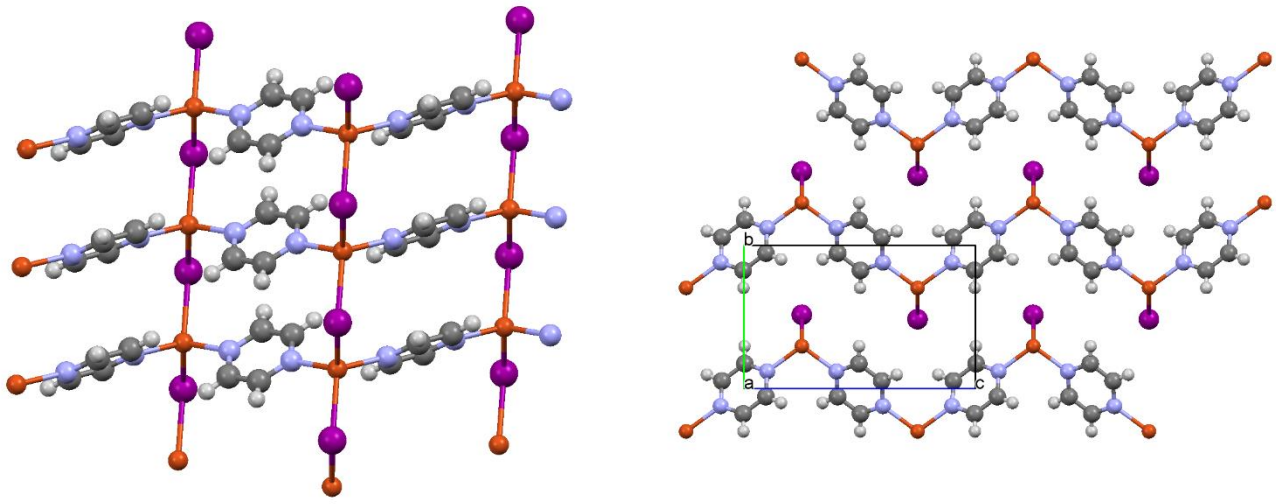

Figure 1 a The 2-D network made of the infinite CuI chain bridged by the pyrazine molecules. b) View along the a-axis, which shows the stratified sheets.

Crystal structure of [Cu$_2$I$_2$(pyz)]$_\infty$

The crystal structure of the polymer [Cu$_2$I$_2$(pyz)]$_\infty$ has already been reported both a T=203K[101] and room temperature.[32] For the sake of the discussion it is worth recalling the salient structural features. The structure of [Cu$_2$I$_2$(pyz)]$_\infty$ is

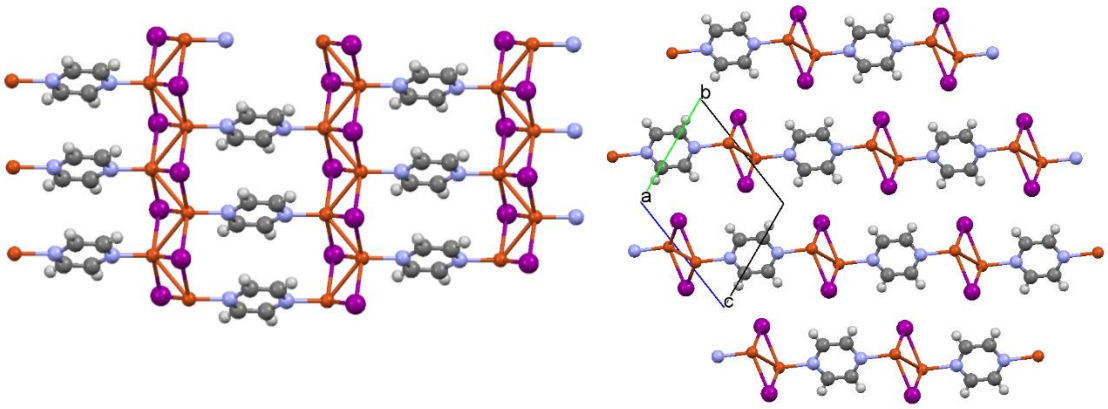

Figure 2 a) The 2-D network made of infinite double CuI Chains bridged by the pyrazine molecules. b) view along the a axis which shows the stratified sheets.

characterized by polymeric double chains in staircase-like arrangements of CuI in which the copper atoms, in tetrahedral coordination, bind three iodine atoms and one pyrazine molecule (fig 2a). Also in this case the ligand acts as a bridge between two adjacent chain forming infinite 2D sheets (fig 2b and c). The Cu-Cu distance 2.7886(6) Å at room temperature which decrease up to is 2.756 (2) Å and at 203 K and it indicates the presence of metallophilic interactions.[28]

Reversible transformation of [CuI(pyz)]$_\infty$ into [Cu$_2$I$_2$(pyz)]$_\infty$

Variable temperature X-ray diffraction confirmed the behaviour observed in the TGA which was similar to that of the isomorphic compounds.[27] The structure of [CuI(pyz)]$_\infty$ is stable up to 100 °C and then releases pyrazine and transforms into the [Cu$_2$I$_2$(pyz)]$_\infty$ crystalline phase over T = 120°C, which is stable up to 175 °C and finally decomposes into CuI (fig 3).

The mechanism of reaction has been hypothesized observing the similarity of the two structures and considering the stoichiometry within the cell. As said

before the structure of $[CuI(pyz)]_\infty$ has a zig-zag configuration while the other one is almost linear so when, at 110 °C, one pyrazine is lost two adjacent chains shrink to form a double chain yielding the complex $[Cu_2I_2(pyz)]_\infty$. Reversibly, when the latter compound is ground with an excess of pyrazine and a drop of acetonitrile, the breakage of the double chain is induced and the structure reverts to the mono chain compound. This transformation is also appreciable by naked eye because of the pronounced difference in the colour of the crystals that switch from the red of $[CuI(pyz)]_\infty$ to the yellow of $[Cu_2I_2(pyz)]_\infty$.

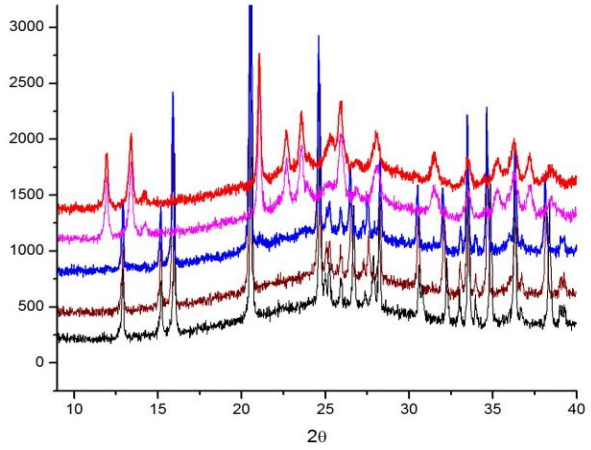

Figure 3 Variable temperature X ray diffraction for $[CuI(pyz)]_\infty$

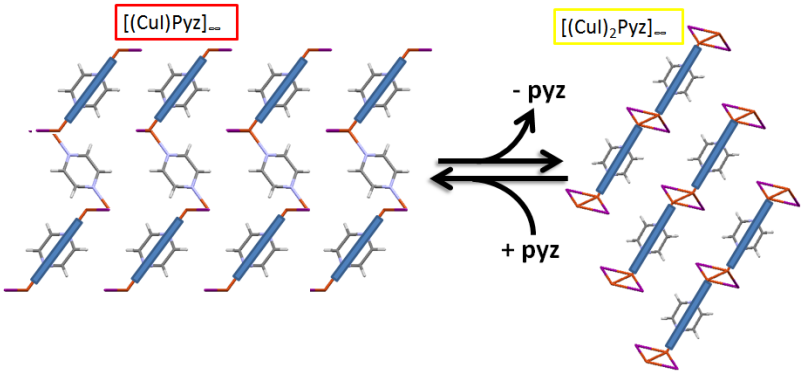

Figure 4. Schematic representation of the mechanism of transformation

Characterization of [(CuI)(pyz)]

[(CuI)(pyz)] can be obtained by grinding with a large excess of pyrazine, 1:4 without presence of acetonitrile, or *via* vapour diffusion but none of these methods led to the formation of crystals suitable for SCXRD. In all cases unreacted CuI was detected. The powder, instead, revealed that is possible to transform this sample into $[Cu_2I_2(pyz)]_\infty$. [(CuI)x(pyz)y] is stable up to a temperature of 90 °C above which it transforms into the $[(CuI)_2pyz]_\infty$ structure. The latter structure is stable up to 200 °C, when the pyrazine begins to sublime leaving only the visible copper iodide at 240 °C (fig 5).

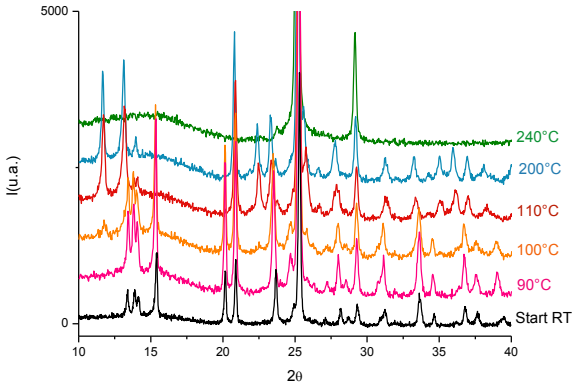

Figure 5: Variable Temperature X ray diffraction evidences the transformation of [CuI(pyz)] in to the pattern of $[Cu_2I_2pyz]_\infty$ and at high temperature into CuI.

[(CuI)x(pyz)y] is quite unstable in presence of small amount of solvent and readily converts into the more stable $[Cu_2I_2(pyz)]_\infty$. The impossibility to wash the compound from the excess of CuI prevents the structural characterization. It is worth noting that by grinding $[Cu_2I_2(pyz)]_\infty$ with an excess of pyrazine but no solvent it is possible to obtain the orange compound [(CuI)x(pyz)y] as summarised in scheme 1.

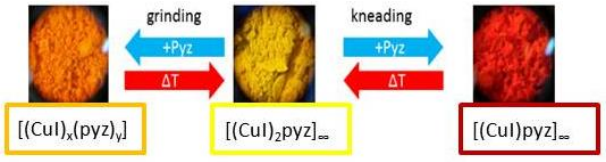

Scheme 1 Solid state transformation of $[Cu_2I_2(pyz)]_\infty$

Photophysical measurements

The luminescence properties of $[CuI(pyz)]_\infty$ and $[Cu_2I_2(pyz)]_\infty$ have been investigated in the solid state both as powders and as single crystals. Emission and excitation spectra at room temperature and 77K are shown in figures 6 and 7 and the relevant data are summarised in Table 2.

Compound $[CuI(pyz)]_\infty$ does not show significant differences in the emission and excitation features when analysed in the two solid forms (Figure 6, top). The room temperature emission is characterized by a broad band peaking at 632/634 nm with a tail extending in the NIR region and the excitation spectrum has a maximum at ca. 530 nm. The Stokes shift is relatively small, of the order 3100 cm^{-1} and the emission quantum yield is of the order of 10% (Table 2). When moving at low temperature, the emission spectrum is red-shifted by ca. 50 nm whereas the excitation spectral features are like those registered at room temperature (Figure 6, bottom). Multi-exponential emission decays are observed both at room temperature and at 77 K. They can be fitted by bi-exponential function with good approximation and a major component (80% of the decay) of the order of 5 and 7 μs is measured for powders and single crystals, respectively, at both temperatures (Table 2).

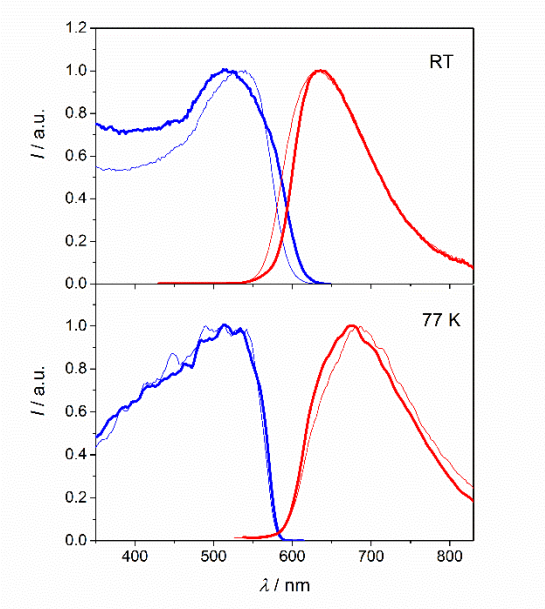

Figure 6: Normalized corrected emission (red, λ_{exc} = 450 nm) and excitation (blue, λ_{em} = 670 nm) spectra of $[CuI(pyz)]_\infty$ (powder sample: thin line; single crystal: thick line) at room temperature (top) and at 77 K (bottom).

Compound $[Cu_2I_2(pyz)]_\infty$ shows peculiar emission properties that depend on the degree of crystallinity of the sample. The single crystals display room temperature emission peaking at 588 nm, with excitation close in energy (Stokes shift of 2200 cm^{-1}; Figure 7, top). The emission decay is dominated by a major component of 2.5 μs (Table 2). At low temperature, a slight bathochromic shift of 16 nm and a hypsochromic shift of ca. 26 nm is observed for emission and excitation spectra, respectively (Figure 7, bottom). For powder samples of $[Cu_2I_2(pyz)]_\infty$, instead, rather different features are observed. The room temperature emission is characterized by a large spectrum peaking at 664 nm and extending far in the NIR. The broad excitation spectrum is confined below 550 nm with maximum at 398 nm, leading to a large Stokes shift of approximately 10000 cm^{-1}. The weak emission (ϕ of the order of 2%) shows a decay that can be fitted by two components with the same weight: 1.8 μs and a much shorter one of 270 ns. At low temperature, the emission spectrum is blue-shifted by 34 nm with respect to the room temperature case, whereas the excitation profile is a broad band with a shoulder at ca. 490 nm (Figure 7). The decay is almost mono-exponential with a lifetime of 12 μs.

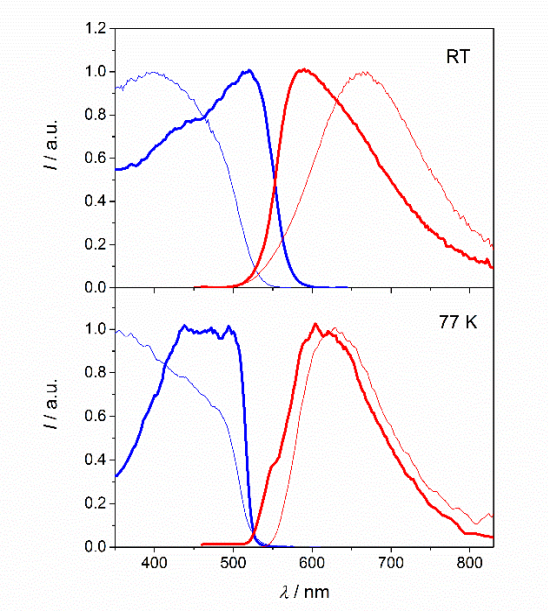

Figure 7: Normalized corrected emission (red, λ_{exc} = 450 nm) and excitation (blue, λ_{em} = 630/670 nm) spectra of $[Cu_2I_2(pyz)]_\infty$ (powder sample: thin line; single crystal: thick line) at room temperature (top) and at 77 K (bottom).

Table 2: Luminescence data at room temperature (RT) and 77 K for powder samples (pd) and single crystals (sc).

		RT			77 K	
		λ_{max} / nm [a]	ϕ [b]	τ / μs [c]	λ_{max} / nm [a]	τ / μs [c]
$[CuI(pyz)]_\infty$	pd632		0.099 ± 0.002	1.2 (30%); 5.0 (70%)	684	1.2 (20%) 5.3 (80%)
	sc 634		-	1.7 (30%); 6.9 (70%)	676	1.5 (25%); 7.5 (75%)
$[Cu_2I_2(pyz)]_\infty$	pd664		0.018 ± 0.001 [e]	0.27 (50%); 1.8 (50%)	630	2.4 (10%); 12.0 (90%)
	sc 588		-	0.66 (20%); 2.5 (80%)	604	- [f] - [f]

[a] Emission maxima from corrected spectra. [b] Absolute emission quantum yields. [c] Emission lifetimes, excitation at 465 nm. [e] At the limit of detection of the system. [f] Weak signal.

CuI coordination polymers containing aromatic ligands have been reported to show luminescence in the 450-600 nm range, which has been attributed either to XLCT (halide-to-ligand charge transfer),[34] XMCT (halide-to-metal charge transfer)[17] or mixed XMLCT (halide/metal-to-ligand charge transfer)[35] transitions. The emission of $[CuI(pyz)]_\infty$ and $[Cu_2I_2(pyz)]_\infty$ in their single crystal form show features that can be ascribed to a ^{3}XMLCT excited state, where the HOMO is a combination of metal and iodide orbitals, delocalized on the CuI infinite chain,[25] and the LUMO is principally based on π* orbitals of the aromatic ligand. The small Stokes shift and the bathochromic shift of the emission observed at low temperature support the hypothesis.[35] Powder samples of $[CuI(pyz)]_\infty$ display emission features like those of the respective crystals (Figure 6), which can be ascribed to the same ^{3}XMLCT excited state. On the contrary, the luminescence of powder samples of $[Cu_2I_2(pyz)]_\infty$ seems to arise from a different excited state. The larger Stokes shift, in particular, points to a ^{3}CC (cluster centred)[20,35-37] nature of the emission, allowed in $[Cu_2I_2(pyz)]_\infty$ where the Cu-Cu distance is below the

sum of the orbital interaction radii (i. e. 2.8 Å). At low temperature, powder samples of $[Cu_2I_2(pyz)]_\infty$ behave similarly to the respective single crystals (Figure 7), suggesting that the observed emission is ^{3}XMLCT in nature. Overall, the data indicate that the population of the ^{3}CC state, lowest in energy, is thermally populated by the higher ^{3}XMLCT in powder samples, but its population is prevented in powders at low temperature and in single crystals. The lack of communication between the excited states in the latter cases can be due to the distortion of the ^{3}CC excited state, which formation is disfavoured in rigid and highly regular structures.

Conclusions

Copper halide coordination polymers have been widely studied because of their interesting luminescent properties. The structures and properties of compounds of general formula $[CuX(pyz)]_\infty$ and $[Cu_2X_2(pyz)]_\infty$ (X= Cl, Br, I) have been reported by several groups with some discrepancies regarding the luminescence characterization. In this part of the thesis I have contributed to the full characterization of the structure of $[CuI(pyz)]_\infty$ which was still unknown. Importantly, in our opinion, the photophysical characterization of crystal and microcrystalline powder of $[Cu_2I_2(pyz)]_\infty$ revealed that the emissive state seems to depend on the crystallinity of the sample. The emissive state in copper iodide compounds is difficult to assign since, depending on the metal-metal distances or on the temperature, it possible to populate different emissive state, i.e. CC vs (X+M)LCT or singlet vs. triplet states.[18] Moreover, the presence of infinite CuI chain opens the possibility to delocalized orbitals.[25] The emission maximum previously reported of $[Cu_2I_2(pyz)]_\infty$ at RT were not consistent (560 nm vs 663nm)[16,17] but they are consistent with our results. The high energy state can be ascribed to the ^{3}XMLCT and the low energy state to the ^{3}CC state. In the microcrystalline $[Cu_2I_2(pyz)]_\infty$ the highly distorted ^{3}CC state can be populated depending on the temperature, while in the crystal of $[Cu_2I_2(pyz)]_\infty$ the population of ^{3}CC state does not take place. Probably, the bigger crystalline domains, which are present in the crystal, prevent the distortion of the CuI double chain and accordingly the population of the ^{3}CC state.

I have also reported the solid state reaction of $[Cu_2I_2(pyz)]_\infty$ which, upon grinding or kneading, can convert into [(CuI)x(pyz)y] and $[CuI(pyz)]_\infty$. The reaction is reversible since upon heating of these latter compound, the $[Cu_2I_2(pyz)]_\infty$ is obtained.

Experimental part

Materials and methods

All glassware was dried in an oven set to a temperature of 80°C for 24h prior to use and stripped with N_2 for 15min. All reagents were purchased from Sigma Aldrich and used without further purification.

Thermogravimetric analysis (TGA)

TGA measurements were performed using a Perkin Elmer TGA7 in the temperature range 35-400°C under N_2 gas flow and heating was carried out at 5°C min^{-1}.

Single crystal Powder Diffraction

Single Crystal Xray Diffraction, (SCXD), were performed on an Oxford Xcalibur S with Mo-Ka radiation, λ= 0.71073 Å, and a monochromator graphite to ascertain the crystalline phase. For structure solution, we used SHELX 97 [6]

Table 1: crystallographic data for compounds $[CuI(pyz)]_\infty$ and $[Cu_2I_2(pyz)]_\infty$

	$[CuI(pyrazine)]_\infty$	$[Cu_2I_2(pyrazine)]_\infty$
Chemical formula	$CuIC_4H_4N_2$	$Cu_2I_2C_4H_4N_2$
Formula Mass	270.54	460.97
Crystal System	Monoclinic	Triclinic
a/Å	4.2688(1)	4.1757(2)
b/Å	6.8827(1)	7.128.(4)
c/Å	11.1738(2)	8.1288(5)
α/°	90	109.64(5)
β/°	96.341(2)	101.807(4)
γ/°	90	96.626(4)
Volume/ Å^3	326.288(11)	218.57
Temperature	RT	RT
Space group	P2/c	P-1
R_{wp}	0.021	0.0553

Variable temperature X-ray powder diffraction

The data were collected in open air in Bragg–Brentano geometry using Cu-Kα radiation without a monochromator. X-ray powder diffractograms were collected in the 2θ range of 5–50° using a Panalytical X'Pert PRO automated diffractometer equipped with an X'Celerator detector and an Anton Paar TTK 450 system for measurements at a controlled temperature.

Photophysics

Determinations made use of powder samples placed inside two quartz slides or single crystals placed on a quartz slide. Room temperature emission and excitation spectra were collected in front-face mode using an Edinburgh FLS920 fluorimeter equipped with a Peltier-cooled Hamamatsu R928 PMT (200–850 nm), and corrected for the wavelength dependent phototube response and light intensity, respectively. 77 K measurements made use of quartz capillary tubes immersed in liquid nitrogen in a cold finger quartz dewar, used in right-angle mode in the same fluorimeter. Absolute emission quantum yields were determined according to the method reported by Ishida et al.,[28] by using a 4 inch Labsphere integrating sphere installed in the same fluorimeter. Each measurement was repeated five times. The limit of detection of the system is 2%. Luminescence lifetimes were measured with an IBH 5000F time-correlated single-photon counting apparatus by using a pulsed NanoLED excitation source at 465 nm. Analysis of the luminescence decay profiles against time was accomplished with the Decay Analysis Software DAS6 provided by the manufacturer, with an estimated error in the lifetimes of 10%.

Synthetic procedures

Synthesis of $[CuI(pyz)]_\infty$

CuI (1 mmol; 0.190 g) and pyrazine (2 mmol; 0.162g) were ground together with few drops of acetonitrile for 20 minutes with a frequency of 20 rev / min. The product is presented as a red crystalline powder. The product was washed with acetonitrile, dried under vacuum and analyzed by X-ray Powder Diffraction. It is also possible to obtain the product with the solvothermal technique. CuI (0,25 mmol; 0,043 g), pyrazine (1 mmol; 0,080 g) and 15 drops of acetonitrile were placed in 8 mL Teflon-lined steel autoclave and heated to 120 °C for 30 mins and then cool down. Squared red crystals were obtained and analyzed by Single Crystal Xray Diffraction.

Synthesis of $[Cu_2I_2(pyz)]_\infty$

The product of $[Cu_2I_2(pyz)]_\infty$ was obtained following the procedure described in literature. [102] CuI (300 mg, 1.57 mmol) dissolved in MeCN (20 mL) was added to

a stirred solution of pyrazine (pyz) (63 mg, 7.9 mmol) in MeCN (20 mL). A yellow precipitate formed immediately and was filtered off after stirring for 1 h. The solid was dried *in vacuo* and analyzed by Xray powder diffraction.
In order to obtain the single crystal of $[(CuI)_2pyz]_\infty$, triple layer reactions were carried out with different solvents as barrier such as dichloromethane, toluene and ethanol and the latter one gave me the best result with crystals suitable for single crystal x ray diffraction.

Synthesis of $[Cu_xI_x(pyz)]$

This compound was mainly synthesized via grinding between the two reagents, with a stoichiometric ratio highly unbalanced towards the ligand (1:4, 1:8) with no further add of solvents. The orange solid obtained was analyzed by Xray powder difraction.

References

1 S. Zhang, Q. Yang, X. Liu, X. Qu, Q. Wei, G. Xie, S. Chen and S. Gao, *Coord. Chem. Rev.*, 2016, **307**, 292–312.

2 B. Li, H.-M. Wen, Y. Cui, W. Zhou, G. Qian and B. Chen, *Adv. Mater.*, 2016, **28**, 8819–8860.

3 H. Zhang, G. Liu, L. Shi, H. Liu, T. Wang and J. Ye, *Nano Energy*, 2016, **22**, 149–168.

4 E. Cariati, E. Lucenti, C. Botta, U. Giovanella, D. Marinotto and S. Righetto, *Coord. Chem. Rev.*, 2015, **306**, 566–614.

5 M. Wallesch, D. Volz, D. M. Zink, U. Schepers, M. Nieger, T. Baumann and S. Br??se, *Chemistry*, 2014, **20**, 6578–6590.

6 A. Barbieri, G. Accorsi and N. Armaroli, *Chem. Commun.*, 2008, 2185–2193.

7 P. C. Ford, E. Cariati and J. Bourassa, *Chem. Rev. (Washington, D. C.)*, 1999, **99**, 3625–3648.

8 M. Wallesch, D. Volz, D. M. Zink, U. Schepers, M. Nieger, T. Baumann and S. Bräse, *Chem. - A Eur. J.*, 2014, **20**, 6578–6590.

9 M. Iwamura, S. Takeuchi and T. Tahara, *Acc. Chem. Res.*, 2015, **48**, 782–791.

10 E. Cariati, E. Lucenti, C. Botta, U. Giovanella, D. Marinotto and S. Righetto, *Coord. Chem. Rev.*, 2016, **306**, 566–614.

11 R. Peng, M. Li and D. Li, *Coord. Chem. Rev.*, 2010, **254**, 1–18.

12 CSD

13 L. Maini, P. P. Mazzeo, F. Farinella, V. Fattori and D. Braga, *Faraday Discuss.*, 2014, **170**, 93–107.

14 D. Braga, F. Grepioni, L. Maini, P. P. Mazzeo and B. Ventura, *New J. Chem.*, 2011, **35**, 339–344.

15 N. M. Khatri, M. H. Pablico-Lansigan, W. L. Boncher, J. E. Mertzman, A. C. Labatete, L. M. Grande, D. Wunder, M. J. Prushan, W. Zhang, P. S. Halasyamani, J. H. S. K. Monteiro, A. de Bettencourt-Dias, S. L. Stoll, P. Shiv Halasyamani, J. HSK Monteiro, A. de Bettencourt-Dias and S. L. Stoll, *Inorg. Chem.*, 2016, **55**, 11408–11417.

16 J. Pospisil, I. Jess, C. Näther, M. Necas and P. Taborsky, *New J.*

Chem., 2011, **35**, 861.

17 F. Farinella, L. Maini, P. P. Mazzeo, V. Fattori, F. Monti and D. Braga, *Dalt. Trans.*, 2016, **45**, 17939–17947.

18 E. Mateo-Martí, L. Welte, P. Amo-Ochoa, P. J. Sanz Miguel, J. Gómez-Herrero, J. A. Martín-Gago, F. Zamora, F. Zamora, Z. C. Mu and G. D. Yang, *Chem. Commun.*, 2008, **13**, 945–947.

19 K. Hassanein, P. Amo-Ochoa, C. J. Gómez-García, S. Delgado, O. Castillo, P. Ocón, J. I. Martínez, J. Perles, F. Zamora, C. J. Goez-García, S. Delgado, O. Castillo, P. Oco, J. I. Martínez, # J Perles and F. Zamora, *Inorg. Chem.*, 2015, **54**, 10738–10747.

20 J. Troyano, J. Perles, P. Amo-Ochoa, F. Zamora, S. Delgado, J. Gómez-Herrero, F. Zamora, C. L. Cahill, J. Pan and M.-C. Hong, *CrystEngComm*, 2016, **18**, 1809–1817.

21 K. Hassanein, J. Conesa-Egea, S. Delgado, O. Castillo, S. Benmansour, J. I. Martínez, G. Abellán, C. J. Gómez-García, F. Zamora and P. Amo-Ochoa, *Chem. – A Eur. J.*, 2015, n/a-n/a.

22 A. Gallego, O. Castillo, C. J. Gómez-García, F. Zamora and S. Delgado, *Inorg. Chem.*, 2011, **51**, 718–727.

23 P. Amo-Ochoa, K. Hassanein, C. J. Gómez-García, S. Benmansour, J. Perles, O. Castillo, J. I. Martínez, P. Ocón and F. Zamora, *Chem. Commun.*, 2015, **51**, 14306–14309.

24 L. Maini, D. Braga, P. P. Mazzeo, L. Maschio, M. Rerat, I. Manet and B. Ventura, *Dalt. Trans.*, 2015, **44**, 13003–13006.

25 A. J. Blake, N. R. Brooks, N. R. Champness, P. A. Cooke, M. Crew, A. M. Deveson, L. R. Hanton, P. Hubberstey, D. Fenske and M. Schröder, *Cryst. Eng.*, 1999, **2**, 181–195.

26 T. Sheets, A. J. Blake, N. R. Brooks, N. R. Champness, P. A. Cooke, M. Crew, A. M. Deveson, L. R. Hanton, P. Hubberstey, D. Fenske and M. Schro, *pergamon*, 1999, **2**, 181–195.

27 P. M. Graham, R. D. Pike, M. Sabat, R. D. Bailey and W. T. Pennington, *Inorg. Chem.*, 2000, **39**, 5121–5132.

28 K. Satoshi, K. Susumu, K. Hitoshi, I. Shinichiro and K. Motomi, *Inorganica Chim. Acta*, 1998, **267**, 143–145.

29 R. Kuhlman, G. L. Schimek and J. W. Kolis, *Polyhedron*, 1999, **18**,

1379–1387.

30 K. Pavani, A. Ramanan and M. S. Whittingham, *J. Mol. Struct.*, 2006, **796**, 179–186.

31 A. M. Goforth, M. D. Smith and H.-C. zur Loye, *J. Chem. Crystallogr.*, 2003, **33**, 303–306.

32 N. Kitada and T. Ishida, *CrystEngComm*, 2014, **16**, 8035–8040.

33 Y. Okano, H. Ohara, A. Kobayashi, M. Yoshida and M. Kato, *Inorg. Chem.*, 2016, **55**, 5227–5236.

34 P. C. Ford and A. Vogler, *Acc. Chem. Res.*, 1993, **26**, 220–226.

35 P. C. Ford, *Coord. Chem. Rev.*, 1994, **132**, 129–140.

36 P. C. Ford, E. Cariati and J. Bourassa, *Chem. Rev*, 1999, **99**, 3625–3647.

37 H. Ishida, S. Tobita, Y. Hasegawa, R. Katoh and K. Nozaki, *Coord. Chem. Rev.*, 2010, **254**, 2449–2458.

Chapter 4

Results of the collaboration with CYNORA Gmbh

Results and discussion

The crystal structure of Cu_3I_3(1,5-bis(diphenylphosphino) pentane)(2-diphenylphosphino-4-methylpyridine$_2$) or (Cu_3I_3(L1)(L2)) was obtained from a yellow crystal with light green luminescence. The complex crystallizes in a monoclinic crystal system with the spatial group $P2_1/c$, lattice parameter a = 19.3768(6) Å, b = 21.2480(5) Å, c = 11.7781(2) Å, β= 97.507(2)° and volume 4807.7 (2) $Å^3$. The structure is characterized by the presence of a rare trimeric Cu_3I_3 unit, which can be described as a planar dimer with a CuI unit added (fig 1a). The ligand L1, which possesses a long aliphatic chain and a P^P bite, forces the Cu2I2 dimer to assume a planar conformation and a Cu2-Cu3 distance of 3.699(1) Å. A similar long Cu-Cu distance is evident in the [Cu_2I_2(L1)$_2$] below (fig 2a, 2b) where the length between the two Cu atoms is forced by the presence of the same aliphatic chain. Among all the possible geometries, the trimeric configuration is the only one which allowed both the ligand to maintain their bite on the same CuI core.

One copper atom interacts with the two others metal atoms and the Cu-Cu distances are (dCu1-Cu3= 2.484(1) Å), (dCu1-Cu2= 2.804(1) Å) and (dCu2-Cu3= 3.699(1) Å). Both ligands bite the same metallic core: the 2-diphenylphosphino-4-methylpyridine ligand coordinates the metal atoms which resembles the classical dimeric core, while the 1,5bis(diphenylphosphino)pentane, which possesses a longer bite, coordinate the most distant copper atoms (figure 1b). Figure 1c shows the packing along the c axes.

a b c

Figure 1: In figure 1a) is shown the trimeric structure of the Cu3I3 core, 1b) shows the whole molecule in which the 2-diphenylphosphino-4-methylpyridine ligand coordinates the metal atoms which resembles the classical dimeric core while the 1,5-Bis(diphenylphosphino)pentane coordinate the most distant copper atoms, 1c) shows the packing along the c axes

The crystal structure of Cu_2I_2(1,5-bis(diphenylphosphino)pentane)$_2$ ($Cu_2I_2(L1)_2$) was obtained from colorless crystal with yellow luminescence. The complex, new and unpublished, crystallizes in a triclinic crystal system with the spatial group P-1 and lattice parameter a = 9.916(5) Å, b = 11.736(5) Å, c = 12.227(5) Å, α=104.456(5), β= 97.565(5)°, γ= 94.721(5) and volume 1356 Å^3. The crystalline structure reveals that the ligand (1,5-bis(diphenylphosphino)pentane binds the Cu atoms to form a planar dimer instead of the classic butterfly-shape core of the compounds characterized by the presence of a P^N ligand. The dimer presents a long Cu-Cu distance (3.659 Å) (fig2a) which is forced by the length of the aliphatic chain. The crystal packing reveals the presence of discrete dimers that show π–π interactions (d= 3.348 Å) between the aromatic rings to form a chain along the c axis (fig 2b).

2a 2b

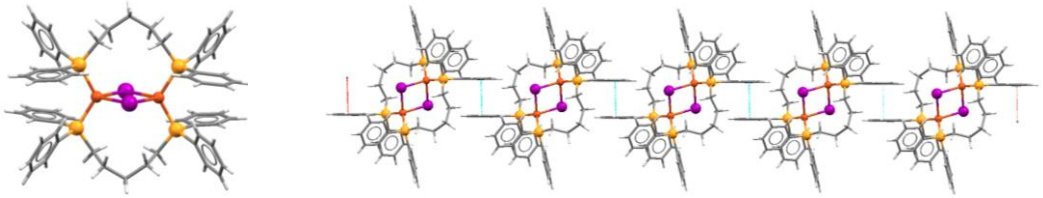

Figure 2: a) Whole molecule of Cu_2I_2(1,5-bis(diphenylphosphino)pentane)$_2$; b) and interactions between the aromatic rings

The powder pattern of the powder as prepared, was collected before recrystallization and compared with the calculated diffratograms of the phase Cu_3I_3 (1,5-bis(diphenylphosphino) pentane) (2-diphenylphosphino-4-methylpyridine$_2$) and Cu_2I_2(1,5-bis(diphenylphosphino)pentane)$_2$.

It is worth noting that the observed pattern presents peaks of both phases plus a third phase which was identified to be the complex Cu_2I_2(2-diphenylphosphino-4-methylpyridine $_2)_3$ [11] as shown in the picture below (fig3).

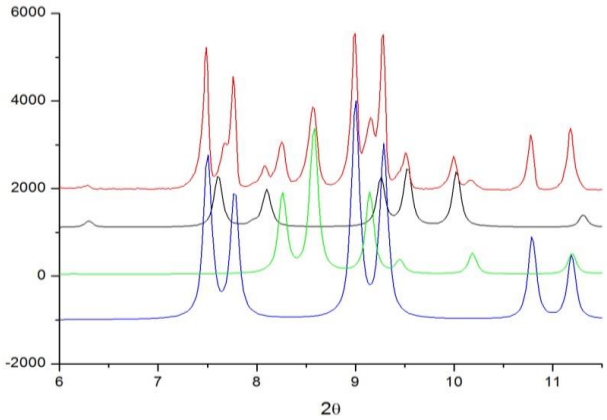

Figure 3: Comparison between the powder pattern of the powder as prapared (red); the calculated pattern of the sample Cu_2I_2(2-diphenylphosphino-4-methylpyridine $_2)_3$ (black); the calculated pattern of the sample Cu_3I_3(1,5-bis(diphenylphosphino)pentane) (2-diphenylphosphino-4-methylpyridine$_2$) (green); the calculated pattern of the sample Cu_2I_2(1,5-bis(diphenylphosphino) pentane)$_2$ (blu).

From a quantitative analysis based on the Rietveld method (fig4) I obtained the percentage of each phase present in the sample. The results of the analysis are summarized in Table 1.

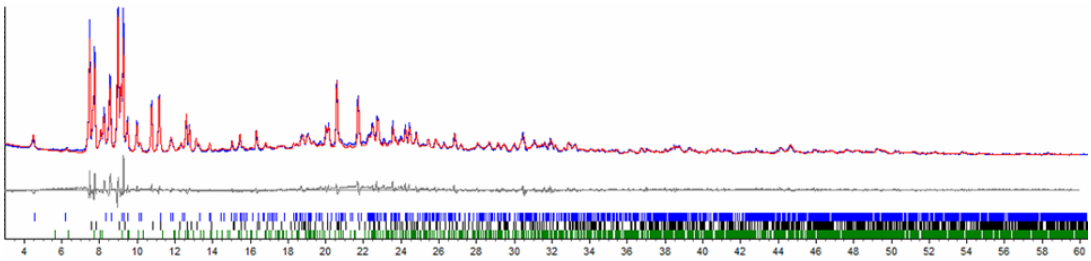

Figure 4: Rietveld analysis of the powder as prepared.

The results of the analysis are summarized in Table 1.

Table 1: Results from the Rietveld refinement

Compound	Percentage (%)
Cu_2I_2(1,5-bis(diphenylphosphino)pentane)$_2$	60
Cu_3I_3(1,5-bis(diphenylphosphino)pentane)(2-diphenylphosphino-4-methylpyridine$_2$)	24
Cu_2I_2(2-diphenylphosphino-4-methylpyridine)$_3$	16

A polimorph phase called Cu_2I_2(2-diphenylphosphino-4-methylpyridine)$_3$ (b) (fig 5) of the sample Cu_2I_2(2-diphenylphosphino -4-methylpyridine)$_3$ (a) was found during the analysis of the sample Maw126 prepared by CYNORA G.m.b.H. The crystal structure reveals a monoclinic crystal system with the space group $P2_1/n$ and lattice parameter a = 14.3451(7)Å, b = 18.9308(13) Å, c = 18.8097(10) Å, α 90, β= 96.585(4)°, γ= 90 and volume 5074.34 Å^3.

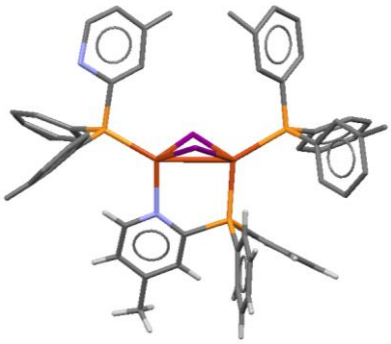

Figure 5: molecule of the polimorph Cu_2I_2(2-diphenylphosphino-4-methylpyridine)$_3$(b) with disorder on the position of the aromatic rings

The structure is characterized by the presence of disorder in the ancillary ligands which does not allow the assigment of the nitrogen atom.

The picture below (fig 6) shows the comparison between the powder pattern of the sample Maw126, red line, and the calculated pattern taken from the structure, blu line.

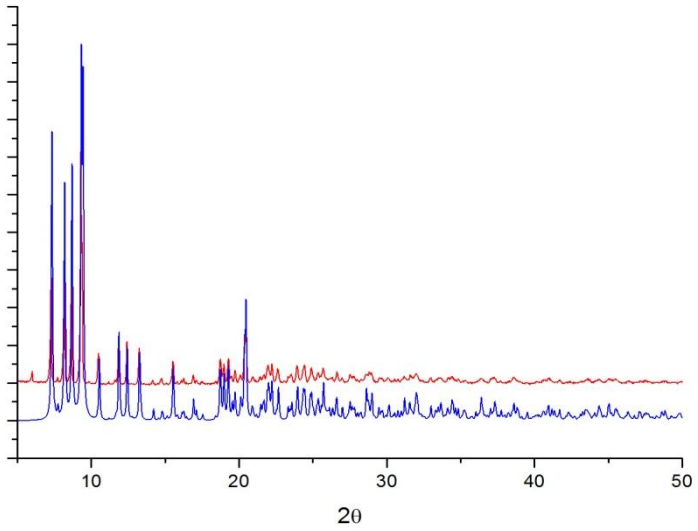

Figure 6: the comparison between the powder pattern of the sample Maw126, red line, and the calculated pattern taken from the structure, blu line.

In the Table 2 the crystallographic rdata of the four complexes are reported.

Table 2: crystallographic details for all the complexes.
L1 is (1,5-bis(diphenylphosphino)pentane); L2 is (2-diphenylphosphino-4-methylpyridine$_2$).

	$Cu_2I_2(L1)_2$	$Cu_3I_3(L1)(L2)$	$Cu_2I_2(L2)_3$ (a)	$Cu_2I_2(L2)_3$ (b)
Chemical formula	$Cu_2I_2C_{58}H_{60}P_4$	$Cu_3I_3C_{47}H_{46}NP_3$	$Cu_2I_2C_{54}H_{48}N_3P_3$	$Cu_2I_2C_{54}H_{48}N_3P_3$
Formula Mass	1261.84	1289		
Crystal System	Triclinic	Monoclinic	Triclinic	Monoclinic
a/Å	9.916(5)	19.37(3)	11.796(1)	14.3451(7)
b/Å	11.376(5)	21.25(3)	15.110(1)	18.9308(13)
c/Å	12.227(5)	11.78(3)	15.770(1)	18.8097(10)
α/°	104.456(5)	90	79.28(1)	90
β/°	97.565(5)	97.5(2)	88.79(1)	96.585(4)
γ/°	94.721(5)	90	68.11(1)	90
Volume/Å^3	1356(29	4807.7(2)	2559.04(2)	5074.3(5)
Temperature	RT	RT	123K	RT
Space group	P-1	$P2_1/c$	P-1	$P2_1/n$
Rwp	0.03	0.05		0.11

Conclusions

The sample cyUbo1 was found to be a mixture of at least three different phases: (Cu_3I_3(L1)(L2)), [Cu_2I_2(L1)$_2$] and Cu_2I_2 Cu_2I_2(L2)$_3$. All of them showed different luminescence and structural properties seen under the UV light at 365nm but not further investigated. The presence of a C5 aliphatic chain in compound Cu_2I_2(L1)$_2$ allowed a longer Cu-Cu distance. The Cu_2I_2(L2)$_3$ compound, form a, was already been published with low a temperature measurement, while I found a polymorphic phase stable at room temperature called form b characterized by the presence of disorder in the ancillary ligands which does not allow the assigment of the nitrogen atom. As already described before, the trimeric structure is not common in the CuI geometric landscape but in this case the geometry is forced by the presence of two ligands with different bite length. The new results presented here are not published but served only to explain the strange luminescent behavior observed in the virgin powder.

Conclusions

The target of my research was to explore the chemistry of CuI with different aromatic N based ligand by varying the stoichiometric ratio and/or the aggregation state.

Six different compounds have been identified with the ligand diphenyl-2-pyridyl phosphine (PN): $[Cu_4I_4(PN)_2]$, $[Cu_4I_4(PN)_2{\cdot}(CH_2Cl_2)_{0.5}]$, $[CuI(PN)_{0.5}]_\infty$, $[CuI(PN)_3]$ whose structures have been determined during this study, $CuI(PN)_2$ which was characterized by powder diffraction data and $[Cu_2I_2(PN)_3]$ which has been already reported. When crystallization by traditional solution procedures failed to give the desired crystal, the crystal structure can be determinate from X-ray powder diffraction data with "direct space" methods. Various examples confirmed that mechanochemistry is a valid route to explore the landscape of the possible structures of CuI derivatives.

Three copper(I) complexes have instead been obtained by the reaction of CuI with 3-picolylamine in acetonitrile solution and characterized by X-ray powder diffraction, both from synchrotron and laboratory radiation. Photophysical investigations in the solid state revealed highly efficient thermally-activated delayed fluorescence (TADF). The complex $[Cu_2I_2(3pica)]_\infty$ displays a strong luminescence thermochromism due to the presence of both ^{1,3}(X + M) LCT excited states and a lower-lying cluster-centered (^{3}CC) one, leading to multiple emission at room temperature; as a result, a white luminescence is achieved with a PLQY of 4.5%. Other three copper iodide coordination polymers have been obtained from the reaction of CuI with pyrazine. The three systems can be recognized on the basis of the different powder color: yellow, red and orange, respectively. By heating up, $[CuI(pyz)]_\infty$ and $[CuI(pyz)]$ convert into $[Cu_2I_2(pyz)]_\infty$, which converts back in to the starting compounds upon kneading or grinding in the presence of pyrazine. The photophysical measurements describe the particular behavior of $[Cu_2I_2(pyz)]_\infty$, the emission maximum at RT can move from 664nm in powder samples to 588nm in crystals. I hypothesized that the two emission band corresponds to two different emissive states and in presence of high crystallinity the low energy band could not be populated.

The sample cyUbo1 was found to be a mixture of three different phases: $(Cu_3I_3(L1)(L2))$, $[Cu_2I_2(L1)_2]$ and Cu_2I_2 $Cu_2I_2(L2)_3$. All of them showed different luminescence and structural properties seen under the UV light at 365nm but not further investigated.

I would also like to sum up all the activities I have been involved in during my Ph.D. period and the paper published in the last three years.
I attended:

- The **"Crystallize COST Action Meeting**, St. Julian, Malta where I gave my contribution with an oral exposition of fifteen minutes.
- The "**X-Ray Scattering Techniques: strategic tools for Material Science**" workshop held at the CNR , Bologna.
- The **"International EXPO/SIR workshop, Crystal structure solution from powders and single crystal: theory and practice"** held in Bari.
- The "**2nd ICSU/IUPAC Workshop on Crystal Engineering"** held in Como where I presented my results by poster presentation.
- The **"48th International School of Crystallography**" held in Erice where I presented my results by poster presentation.
- The **"XLIV Congresso Nazionale di Chimica Inorganica"** where I gave my contribution with an oral exposition of fifteen minutes.

I also attended the 8th editions of the workshop **"Crystal forms: Crystals in Food & Pharma"** held in Bologna. I spent a 5 months period at the University of Nottingham under the supervision of Prof. Neil Champness.

The list of publications is reported below:

- F. Farinella, L. Maini, P. P. Mazzeo, V. Fattori, F. Monti and D. Braga, *Dalt. Trans.*, 2016, **45**, 17939–17947.
- L. Maini, P. P. Mazzeo, F. Farinella, V. Fattori and D. Braga, *Faraday Discuss.*, 2014, **170**, 93–107
- L. Maini, F. Farinella, B. Ventura, D. Braga "Some highlights on the luminescent properties of mono and double chain structures of the Copper Iodide and pyrazine coordination polymers" ***in preparation.***

Appendix A

White luminescence achieved by a multiple thermochromic emission in a hybrid organic–inorganic compound based on 3-picolylamine and copper(I) iodide

TGA analysis of [Cu_2I_2(3pica)]∞

The TGA analysis of [Cu_2I_2(3pica)]∞ (Fig 1) reveals that the complex is stable up to 210°C which corresponds to decomposition temperature. No other crystalline phases have been detected. Both of the losses below 400°C were assigned to the release of the ligand.

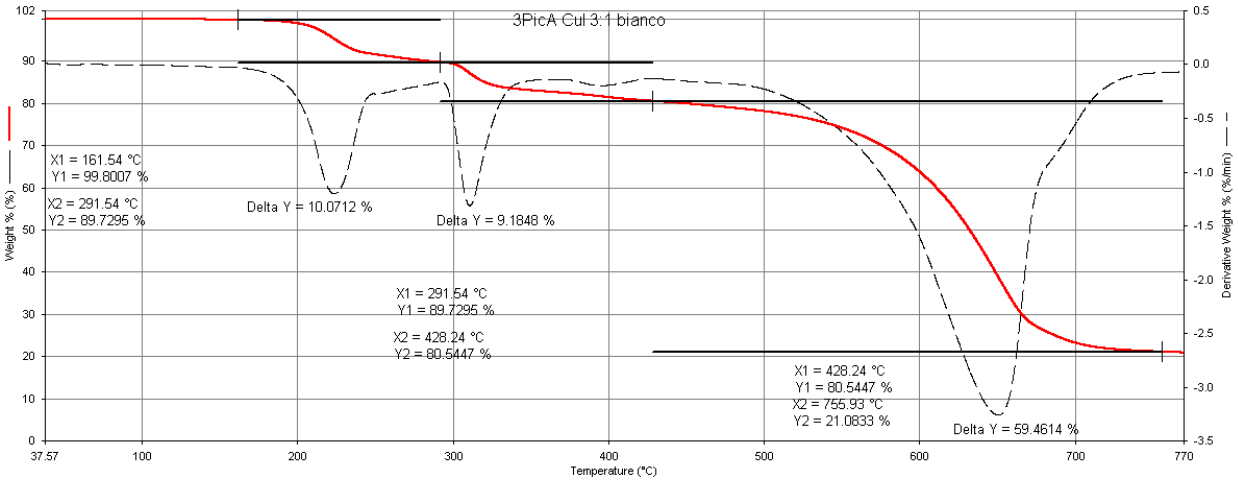

Fig. 1: TGA analysis of crystalline Cu_2I_2(3pica)∞

TGA analysis of [CuI(3pica)]

The TGA analysis of the complex [CuI(3pica)] (fig 2a) shows a first weight loss of 17.7% which corresponds to the release of one ligand. From the variable temperature XRPD (fig 2b) I have indications of the thermal stability of the complex, in fact a progressive decomposition of the powder is observed, up to the amorphization which occurred at 170 °C.

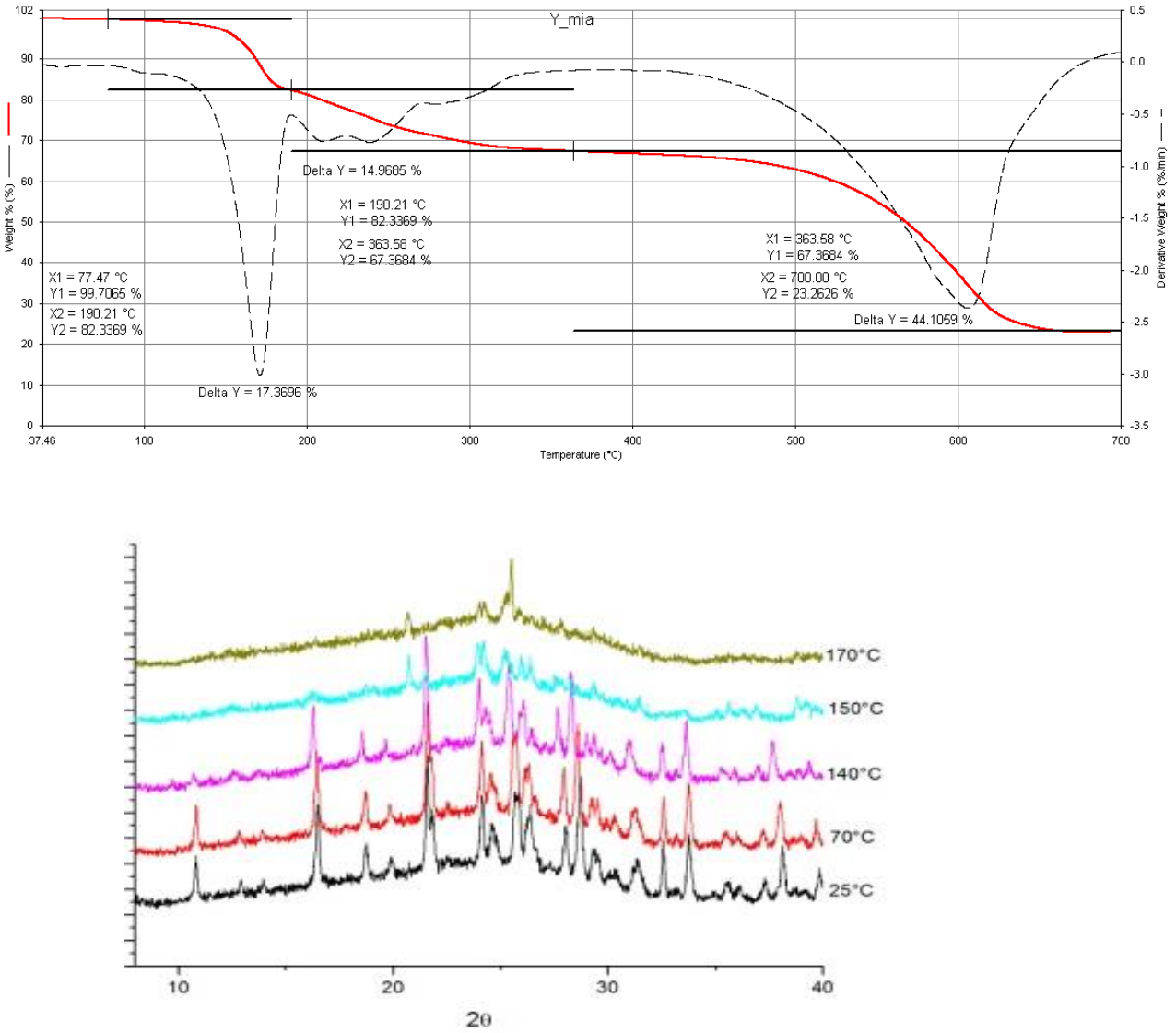

Fig. 2: a) TGA of crystalline [CuI(3pica)]; b) comparison of the powder pattern at different temperature for crystalline [CuI(3pica)].

TGA analysis of [CuI(3pica)](CH₃CN)

The TGA analysis of the complex [CuI(3pica)] (CH_3CN) (fig 3a) shows a total weight loss of 37%, below 300°C, which corresponds to the release of the solvent and the ligand. From the variable temperature XRPD (fig 3b) I have indications of the thermal stability of the complex, in fact a progressive decomposition of the powder is observed, up to the amorphization which occurred at 170 °C together with the loss of the solvent.

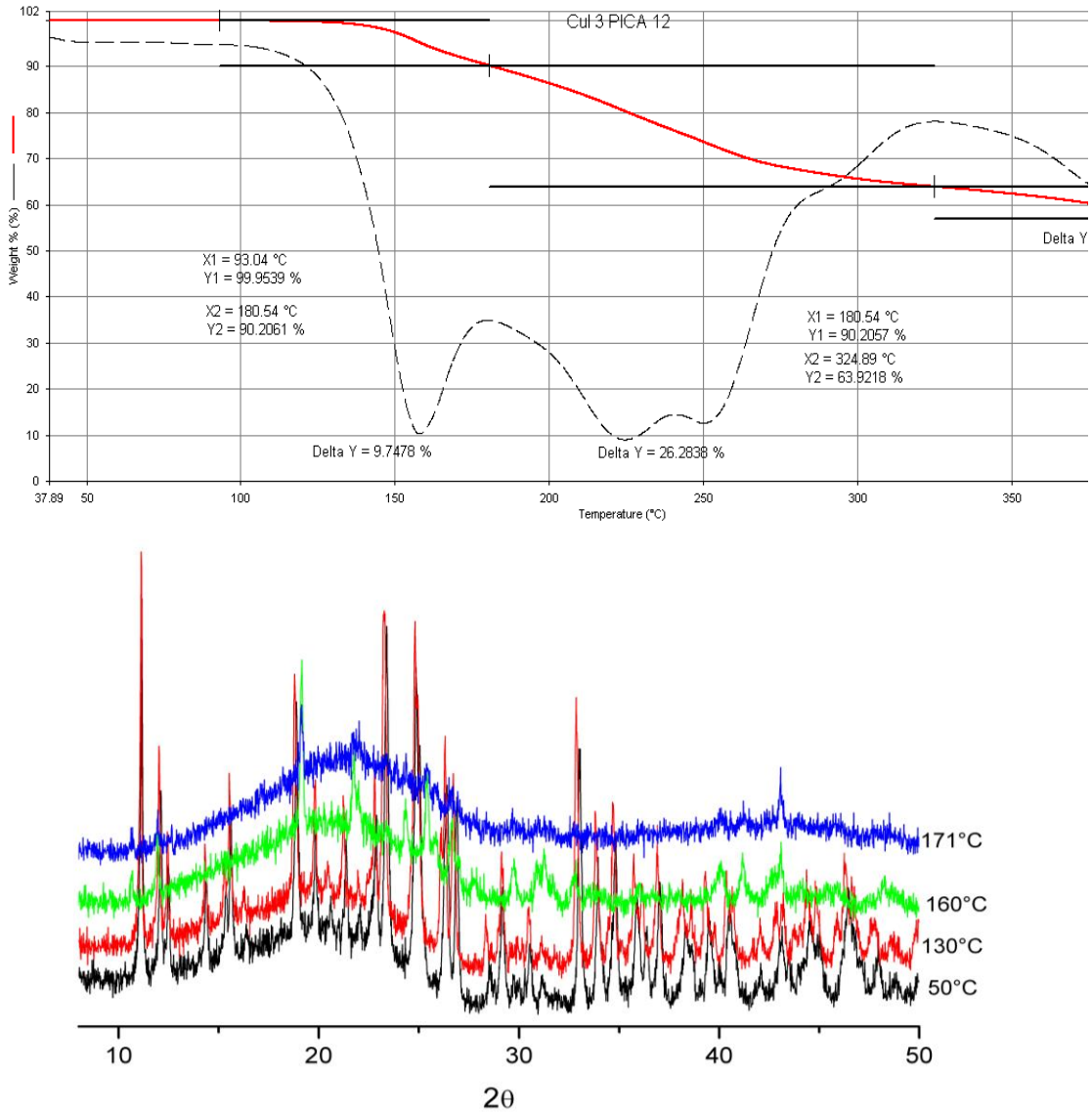

Fig. 3: a) TGA of crystalline [CuI(3pica)]; b) comparison of the powder pattern at different temperature for crystalline [CuI(3pica)] (CH_3CN).

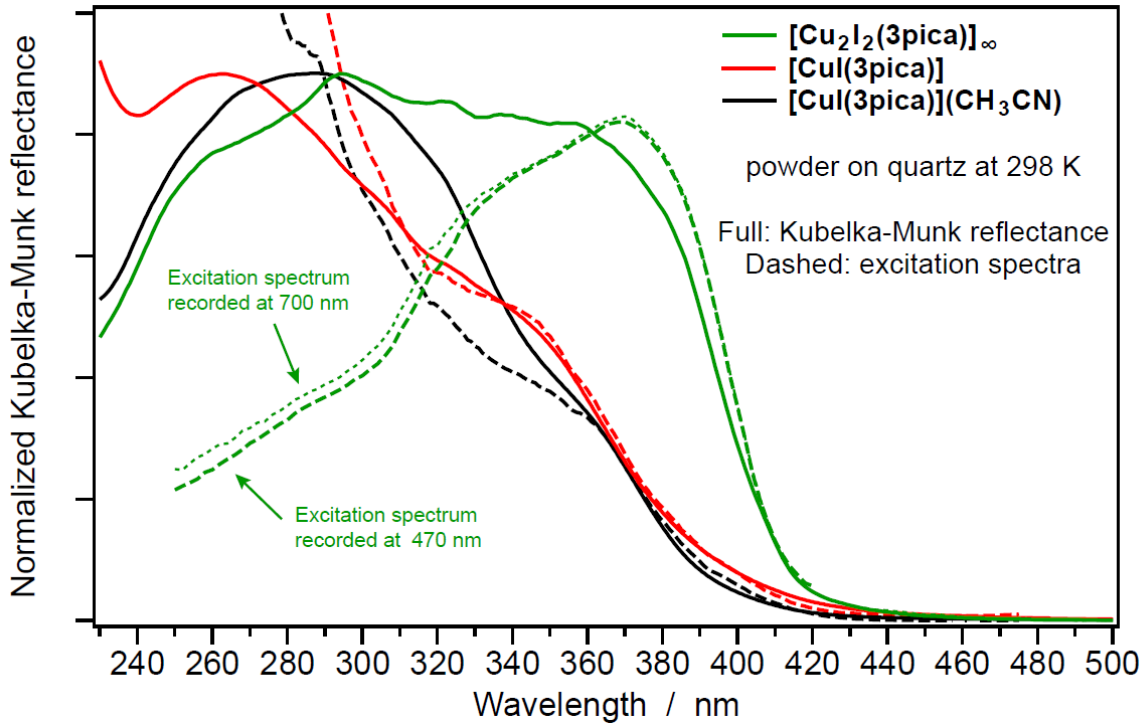

Fig. 4: Comparison between the diffuse reflectance spectra (elaborated using the Kubelka-Munk function) and the excitation spectra of all the investigated Cu(I) complexes in solid state, as neat powder on quartz slides. All the excitation spectra were recorded at emission maximum, except for the white-emitting complex [CuI(3pica)](CH$_3$CN). In that case, two different emission wavelengths were selected (*i.e.*, one on the ^{1,3}(X+MLCT) and the other on the ^{3}CC band) in order to rule out the presence of emitting impurities.

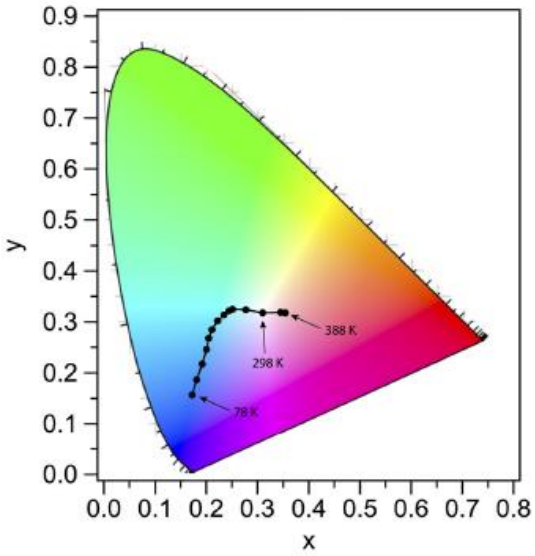

Fig 5: Variation in the emission color of $Cu_2I_2(3pica)_\infty$ with temperature. The CIE coordinates on the chromaticity diagram are calculated from the corrected emission spectra reported in Fig 7 of the main text.

Appendix B

Some highlights on the luminescent properties of mono and double chain structures of the Copper Iodide and pyrazine coordination polymers.

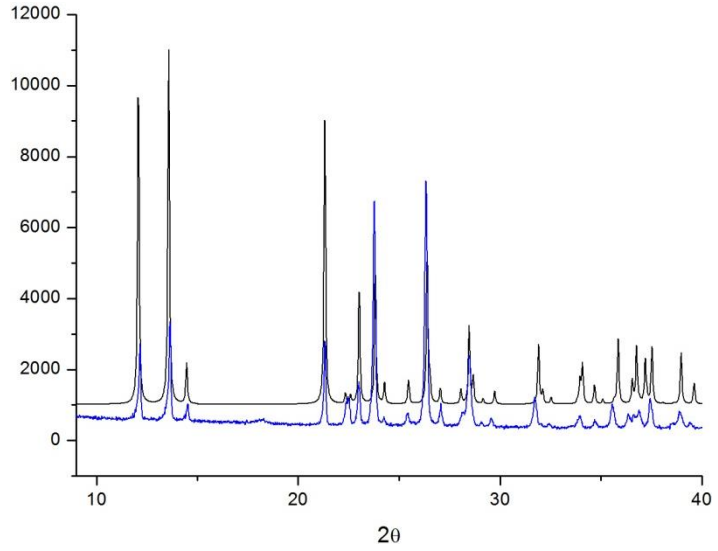

Figure 1: comparison between the XRPD diffrattogramm of $Cu_2I_2(pyz)_\infty$ experimental (Blue) and $Cu_2I_2(pyz)_\infty$ calculated from the structure (Black)

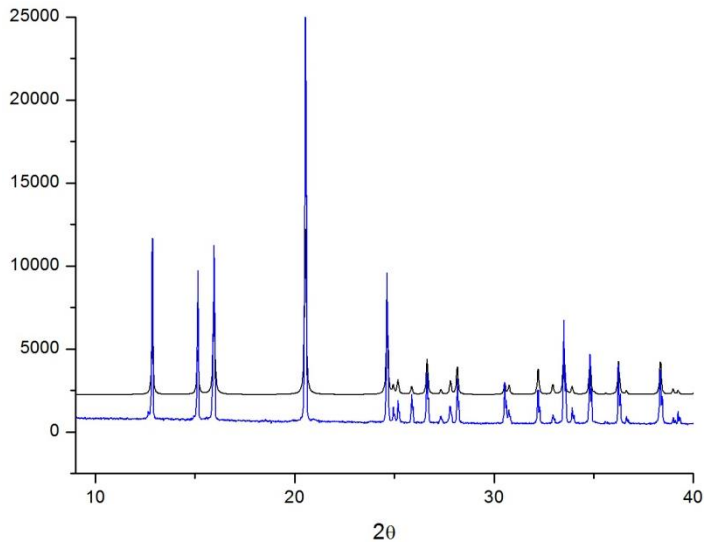

Figure 2: comparison between the XRPD diffrattogramm of $CuI(pyz)_\infty$ experimental (Blue) and $CuI(pyz)_\infty$ calculated from the structure (Black)

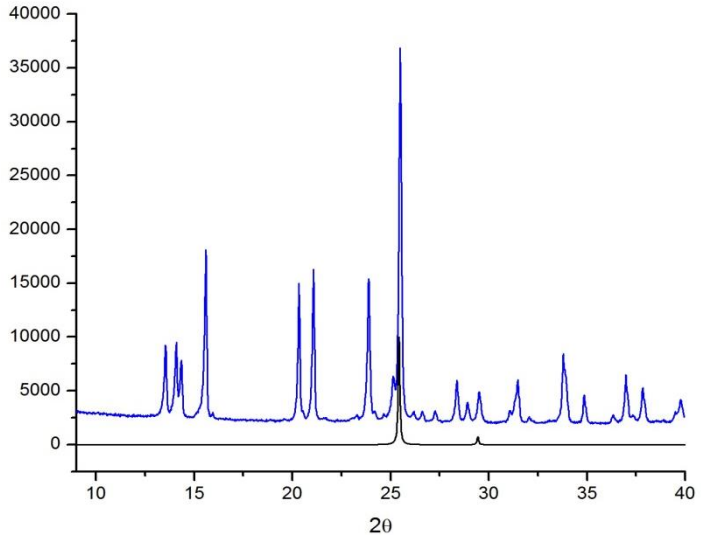

Figure 3: comparison between the XRPD diffrattogramm of Cu_xI_y(pyz) experimental (Blue) and CuI calculated from the structure (Black)